

M.S-I

STUDY OF SHORT TERM PHASE STABILITY

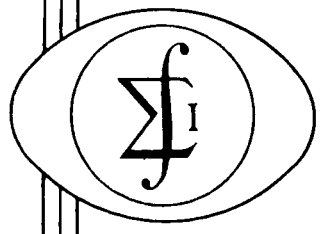
GPO PRICE \$ _____
 CFSTI PRICE(S) \$ _____
 Har. copy (HC) _____
 Microfiche (MF) _____

ff 653 July 65

SMITH ELECTRONICS, INC
Cleveland 41, Ohio

INTERIM REPORT

MARCH 16, 1964 THRU MARCH 16, 1965



FACILITY FORM 602

N67 12270
(ACCESSION NUMBER)
57
(PAGES)
CR-80091
(NASA CR OR TMX OR AD NUMBER)

(THRU)
1
(CODE)
07
(CATEGORY)

CONTRACT NO NAS 8-11592

MARSHALL SPACE FLIGHT CENTER
NATIONAL AERONAUTICS AND SPACE ADMINISTRATION
HUNTSVILLE, ALABAMA

CONTENTS

ABSTRACT	iv
1. INTRODUCTION	1
2. STUDY OF FREQUENCY DIVISION	1
2.1 Basic Divider Concepts	2
2.1.1 The Distinction Between Signal and Noise	2
2.1.2 Instructing the Operator	3
2.2 Analytical Approaches	3
2.2.1 Statistical Method	3
2.2.2 Models Derived from Power Series Consideration	4
2.2.3 Dividers, Bandwidth, and Time - Another Model	10
2.2.4 Practical Dividers	11
2.2.5 A Carrier Divider	11
2.3 Effect of Division on Sine and Random Function	12
2.3.1 The Action of a Frequency Divider Defined	12
2.3.2 The Action of a Divider on a Sine Wave Plus Noise	13
2.3.3 The Action of a Divider on a Band Limited Random Function	14
2.3.4 Effect of Divider on Spectra	16
2.3.5 Conclusions	21
2.4 Application of Step-Recovery Diode to Division	21
2.4.1 Manley-Rowe Frequency - Power Relation	21
2.4.2 Switch Energy - Power Relation	22
2.4.3 Quantum Mechanical Basis for Energy - Power Formulas	22
2.4.4 Mechanism of Subharmonic Generation	23
2.4.5 Experimental Subharmonic Generation	23
3. RF AMPLIFIER PROGRAM	28
3.1 Parametric Amplifier Study	28
3.1.1 Description of Types	28
3.1.2 Characteristics	32
3.1.3 Stability Considerations	35
3.1.4 Choice of Type of Parametric Amplifier	36

CONTENTS (continued)

3.2	Tunnel Diode Down-Conversion	37
3.2.1	Balanced Micro-strip Design	37
3.2.2	Balanced Coaxial Hybrid Design	37
3.2.3	Strip Line Version	40
3.2.4	Observations	42
4.	REVIEW OF PHASE STABILITY MEASUREMENT PROCEDURES	45
4.1	Description	45
4.2	Analysis of System	45
4.3	Observations	48
5.	SUMMARY	50
6.	RECOMMENDATIONS	50
7.	REFERENCES	51

Table 1	Comparison of Conventional Types of Parametric Amplifiers	34
---------	---	----

FIGURES

1.	DIVISION BY TWO WITH AN IDEAL TRANSFER FUNCTION	5
2.	DIVISION BY TWO WITH A "PRACTICAL" TRANSFER FUNCTION	6
3.	THE EFFECT OF A DIVIDER ON WHITE NOISE	17
4.	THE EFFECT OF A DIVIDER ON THE SPECTRAL DENSITY OF AN ARBITRARY FUNCTION	18
5.	THE EFFECT OF A DIVIDER ON A SERVO AND COMMUNICATIONS RANDOM FUNCTION	19
6.	THE EFFECT OF A DIVIDER ON THE SPECTRAL DENSITY OF THE RANDOM FUNCTION OF FIG. 5	20
7.	SCHEMATIC OF REVISED $\frac{1}{13}$ SUBHARMONIC GENERATOR	25
8.	$\frac{1}{13}$ SUBHARMONIC GENERATOR USING CHARGE-STORAGE DIODE	27
9.	SPECTRUM DISPLAY OF MODULATED CARRIER	29
10.	SETUP FOR MODULATION TEST OF SUBHARMONIC GENERATOR	30
11.	PHASE STABILITY MEASUREMENT SET-UP	31
12.	MICRO-STRIP BALANCED TD DOWNCONVERTER	38

FIGURES (continued)

13.	BALANCED COAXIAL DOWNCONVERTER	39
14.	STRIP LINE TUNNEL DIODE DOWNCONVERTER	41
15.	STRIP LINE DOWNCONVERTER	43
16.	DIODE MOUNTING FOR STRIP LINE DOWNCONVERTER	44
17.	SCHEMATIC OF HYBRIDGE AND SUMMING NETWORK FOR PHASE JITTER MEASUREMENT SYSTEM	46

ABSTRACT

12270

Theoretical and experimental work in the area of frequency division is reported. It is shown that true frequency division is a rarity because of the requirement for storage capability. Examination of various models indicates that signal-to-noise enhancement by the frequency division operation per se is not possible. Experimental subharmonic generation with step-recovery diodes is reported.

A survey of types of parametric amplifiers is presented and experimental work with tunnel diodes as L- and S-band downconverters described. It is concluded that noise figure results comparable to or slightly better than high quality crystal diodes are achievable with an advantage in low L.O. power requirement.

A review of the theory of one approach to phase stability is included.

Author

INTERIM REPORT COVERING WORK DONE ON CONTRACT NAS 8-11592
MARCH 16, 1964 THROUGH MARCH 16, 1965

1. INTRODUCTION

Work done by Smith Electronics, Inc. on Contract NAS 8-11592 for Geo. C. Marshall Space Flight Center of NASA has been conducted along two major lines; the study of frequency division with both theoretical and experimental programs; and a UHF RF amplification investigation with parametric amplifier and tunnel diode down conversion phases. The study of frequency division has included general theoretical study as well as analysis of specific problems. Experimental work has been conducted with subharmonic generation.

The RF amplification program consisted of a general study of parametric amplification and experimental work with tunnel diodes as down-converters.

Three special reports were issued during the 12 month period covered by this report disclosing results of the theoretical study of frequency division. The first and third reports, dated June 12 and December 7, 1964, dealt with the general theory of frequency division, and the second, dated September 28, 1964 was limited to the theory of subharmonic generation. Some of the material in these reports is reproduced here; additional work is also covered.

2. STUDY OF FREQUENCY DIVISION

The initial phase of the divider study was directed toward determining the effect of a hypothetical true frequency divider on the signal-to-noise ratio of an input. An analytical approach was undertaken followed by mathematical study of a sine wave plus random noise. An effort was made to find such a hypothetical divider and practical divider circuits were considered in the light of the theoretical conclusions, with particular emphasis on the snap-off or step-recovery diode as a subharmonic generator.

The hypothetical true frequency divider was defined as having the following properties.

a. It divides the frequency of the incoming signal and preserves the amplitude unchanged.

b. If the incoming signal is analyzed as sinusoidal components, each component's amplitude is unaltered and its frequency is divided by the same integer. Provisionally, the division process is extended to include angle as well as frequency.

2.1 Basic Divider Concepts

There are two concepts concerning the division problem which are being proffered as fundamental principles.

a. In order for any operator (human or machine) to improve signal-to-noise ratio, the signal must be distinguishable from the noise by some property or properties.

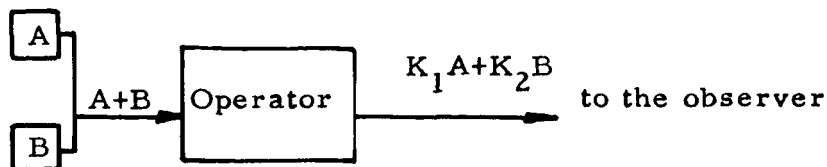
b. In order for any operator (human or machine) to improve signal-to-noise ratio, the operator must receive instructions (these instructions may be in the form of programming or design parameters) as to the distinction between signal and noise.

Improving the signal-to-noise ratio is identically the same as improving the ratio of the desired to the undesired signal; is identically the same as improving the order of the system; is identically the same as reducing the entropy of the system. Proofs of these propositions will be given using electrical analogies.

2.1.1 The Distinction Between Signal and Noise

The operator or processor is shown as a two-port having at the input two signals, A and B (it is known only to the observer that A is the signal and B is noise) and at the output A and B, modified perhaps.

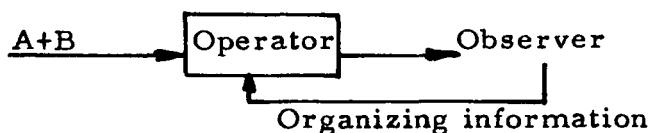
For example, A could be the thermal voltage



from a resistor in one compartment and B is the thermal voltage from another resistor in a separate compartment. They arrive by the same transmission medium. The observer is interested in A, and only because of this interest does A become signal and B noise. The operator is interposed to increase the ratio $\frac{A}{B}$.

2.1.2 Instructing the Operator

Let us hypothesize an operator which increases $\frac{A}{B}$; by what mechanism is not material. Then one would say the signal-to-noise ratio had been increased. If another observer is interested in B, the operator has reduced the signal-to-noise ratio because B now becomes signal and A noise. This uncertainty is absurd and it shows that no device can improve signal-to-noise ratio without an input from the observer designating signal and noise. The observer cannot make this designation without first distinguishing one signal from the other. Then the operator should be shown as



2.2 Analytical Approaches

Many analytic techniques are available as standard, accepted tools for calculating the effect a device or network has on any signal which is passed through it. Those techniques which are limited to the study of deterministic inputs or linear circuits were not considered at all. Models of dividers were sought to help guide this study.

2.2.1 Statistical Method

Usually the effect of a linear two-port on the statistics of a signal may be determined by using its transfer function

$$H(j\omega) = \frac{Y(j\omega)}{X(j\omega)} \quad (1)$$

This is the "single valued" ratio of the output amplitude to the input amplitude as a function of ω . The probability density function of the output is

$$p_2 [y(t)] = p_1 [x(t)] \frac{dX}{dY} \quad (2)$$

But in the divider the amplitude ratio is constant. Then

$$p_2 [y(t)] = p_1 [x(t)] \quad (3)$$

and it appears the statistics of the signal are unchanged by the assumed divider.

If the signal may be expressed as the sum of a series of terms generally of the form $a_n \sin \psi_n$ where

$$\psi_n = (\omega_n t + \phi) \quad (4)$$

and a_n is constant with time, the information is carried by ψ . If this signal is the input to a divider of ratio m , the output is $a_n \sin \theta_n$ where $\theta_n = \frac{\psi_n}{m}$.

The information transfer function is the angle (ψ_n) transfer function and is a constant $\frac{1}{m}$. Then this approach also shows no change in the probability density function of the signal.

For clarification, sketches have been made of the required transfer functions to accomplish frequency division of a single sine wave. All of these transfer functions are variable with time and have plus and minus infinities. For example, Fig. 1 shows division by two, with an ideal transfer function. It is seen that the required transfer function must go to infinity at the downward zero-crossings of the input signal.

If the transfer function is finite, the result is shown in Fig. 2.

2.2.2 Models Derived from Power Series Considerations

An analytic model of the divider has been sought. This model must be perfectly general to be useful. The utility of a model arises from being able to apply a signal to the divider, and by determining the output, to obtain a transfer function for the divider. This transfer function will show the influence of the divider on the statistics of the signal.

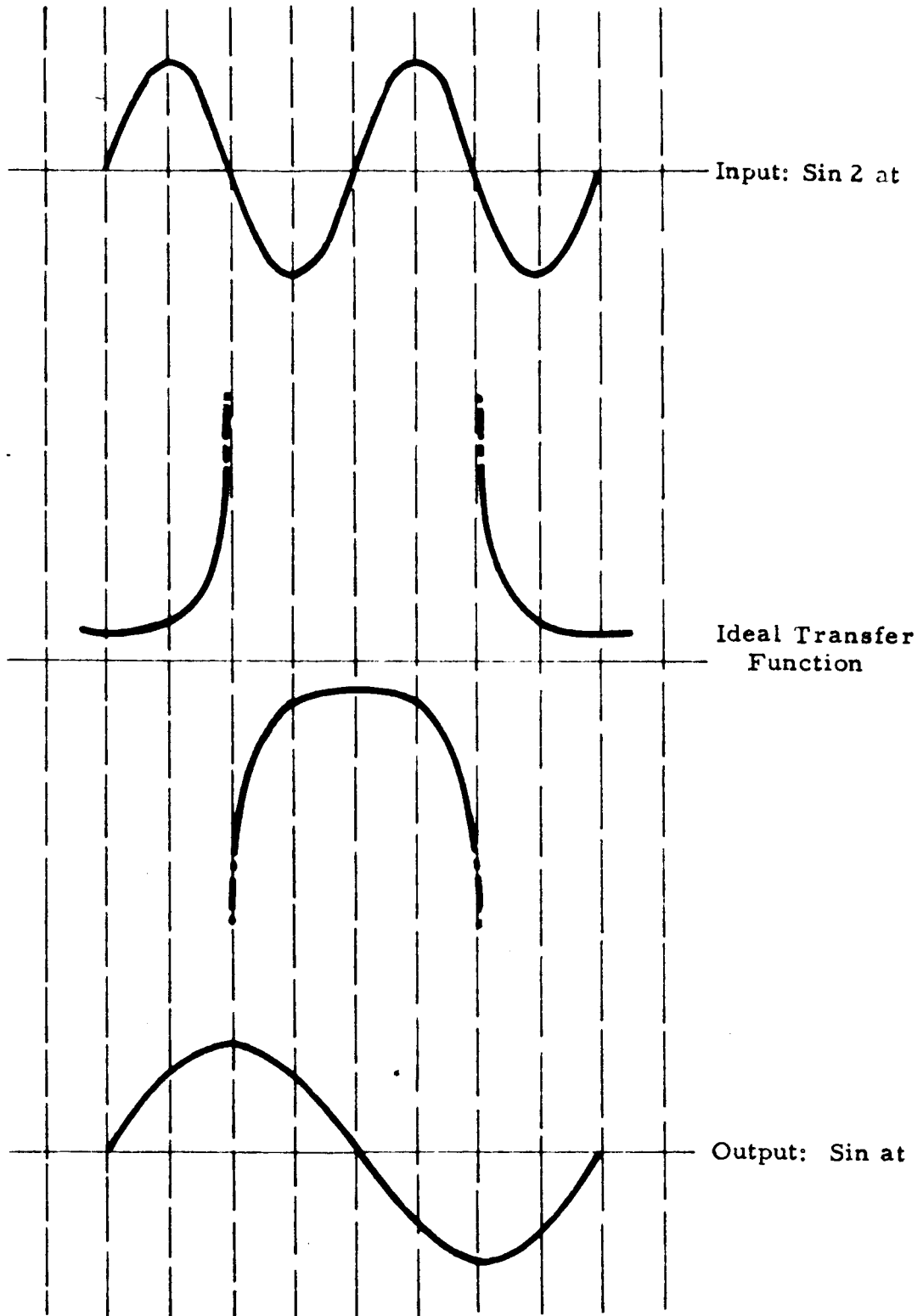


FIG. 1 DIVISION BY TWO WITH AN IDEAL TRANSFER FUNCTION



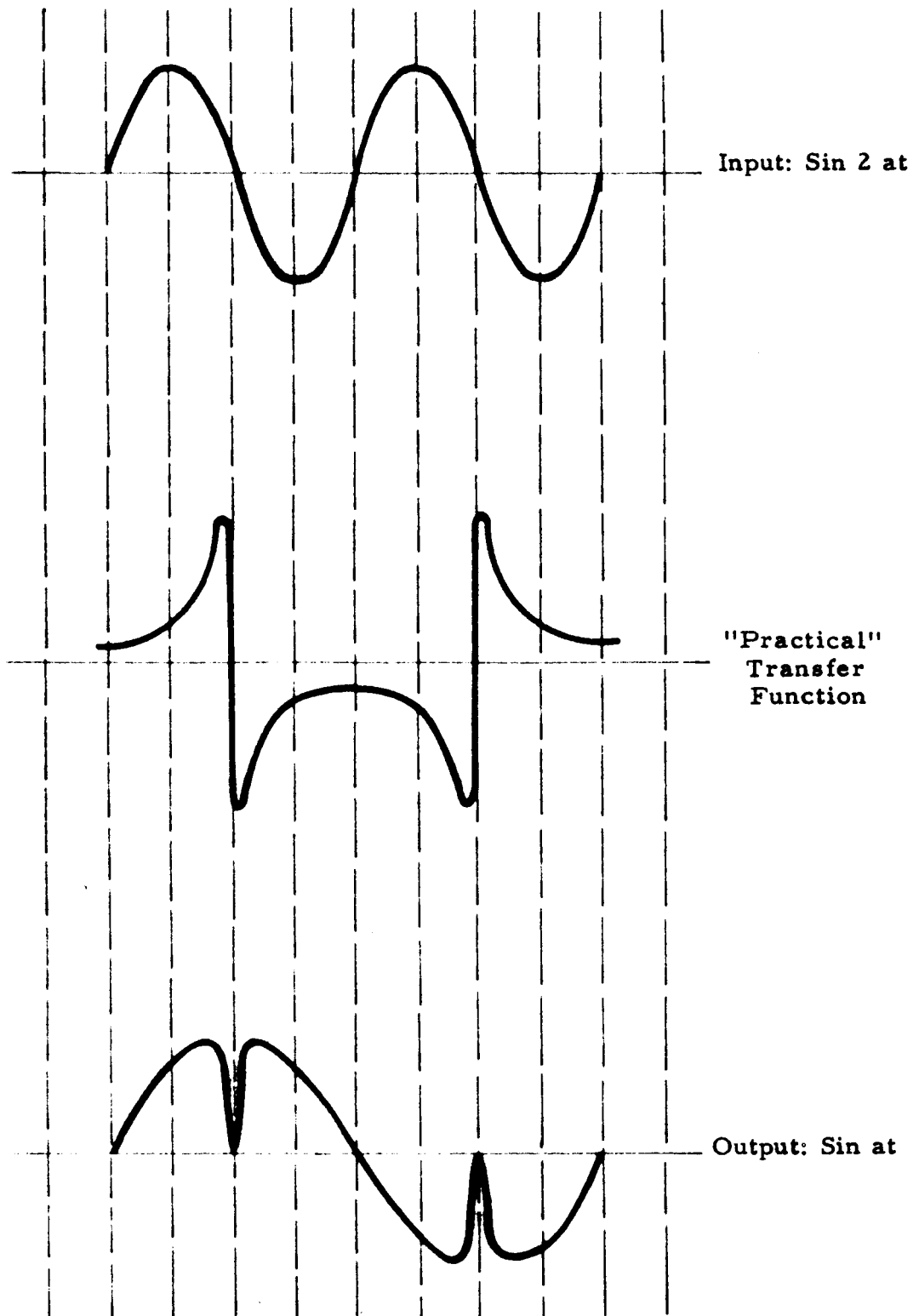


FIG. 2 DIVISION BY TWO WITH A
"PRACTICAL" TRANSFER FUNCTION



One approach is based on a power series expansion of a sinusoidal waveform in terms of its subharmonic. Four models are developed using operational amplifiers, rooting and raising to a power, which are practical approaches. These are not meant to indicate a direction for an experimental program but only as analytical aids.

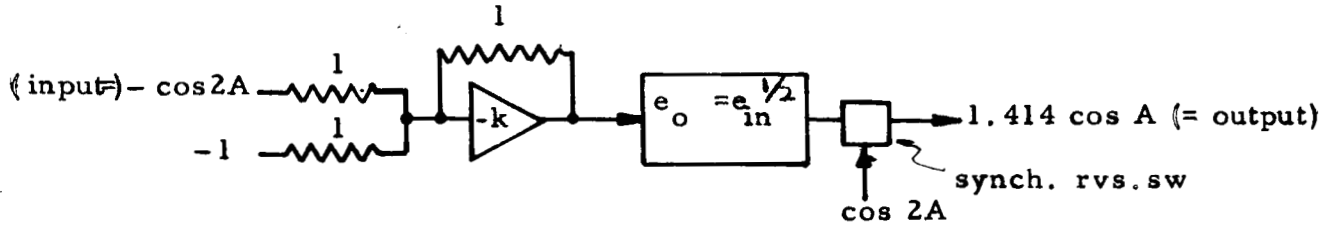
An expansion for $\cos n A$ is

$$\begin{aligned} \cos nA &= 2 \frac{(n-1)}{1!} \cos^n A - \frac{n}{1!} 2 \frac{(n-3)}{2!} \cos^{(n-2)} A \\ &+ \frac{n(n-3)}{2!} 2 \frac{(n-5)}{3!} \cos^{(n-4)} A - \frac{n(n-4)(n-5)}{3!} 2 \frac{(n-7)}{4!} \cos^{(n-6)} A \\ &+ \frac{n(n-5)(n-6)(n-7)}{4!} 2 \frac{(n-9)}{5!} \cos^{(n-8)} A \dots \dots \end{aligned} \quad (5)$$

(a) One special case is, for $n = 2$,

$$-\cos 2A = -2 \cos^2 A + 1 \quad (6)$$

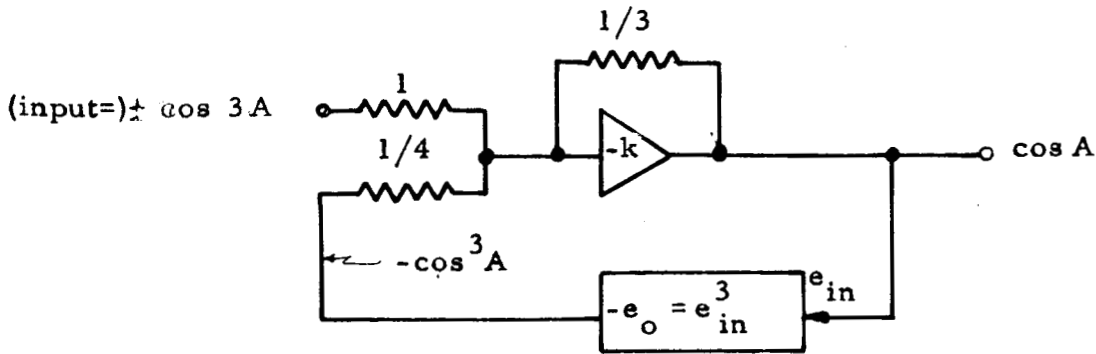
This may be instrumented as shown below for divider action.



(b) Another special case is, for $n = 3$,

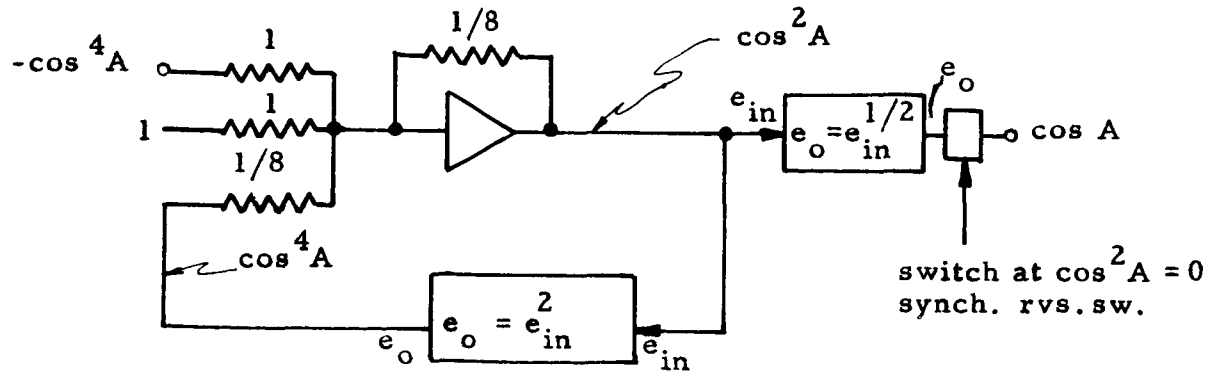
$$\cos 3A = 4 \cos^3 A - 3 \cos A \quad (7)$$

This may be instrumented for divider action as shown.



(c) For $n=4$ (a division ratio of four)

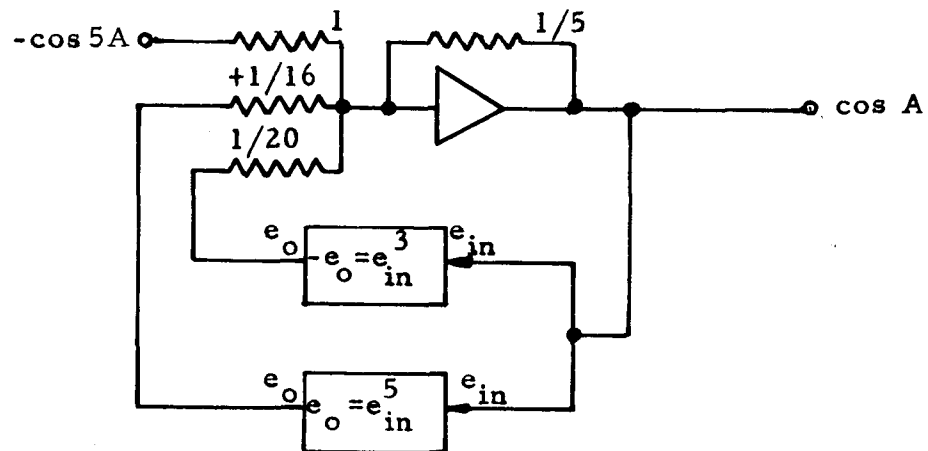
$$\cos 4A = 8 \cos^4 A - 8 \cos^2 A + 1 \quad (8)$$



It may be noted that only even ordered dividers need the synchronous reversing switch to obtain proper polarity on the negative half-cycles.

(d) For $n=5$ (a division ratio of five)

$$\cos 5A = 16 \cos^5 A - 20 \cos^3 A + 5 \cos A \quad (9)$$



The outputs of these dividers are related to the inputs in a manner that makes it impossible to analyze with an arbitrary input. Reversion of the series is a direct approach but requires too many terms to be useful. Another approach also yields a solution:

Rewriting Eq. (7) as

$$4e_o^3 - 3e_o - e_{in} = 0$$

$$\text{We solve, equivalently, } e_o^3 - \frac{3}{4}e_o - \frac{e_{in}}{4} = 0$$

(10)

Korn & Korn, *Mathematical Handbook for Scientists and Engineers* p.23 gives

The roots of $y^3 + py + q = 0$ are

$$A+B, -\frac{A+B}{2} \pm j \frac{A-B}{2} \sqrt{3}$$

$$\text{where } A = \sqrt[3]{-\frac{q}{2} + \sqrt{\left(\frac{p}{3}\right)^3 + \left(\frac{q}{2}\right)^2}} \quad (11)$$

$$B = \sqrt[3]{-\frac{q}{2} - \sqrt{\left(\frac{p}{3}\right)^3 + \left(\frac{q}{2}\right)^2}} \quad (12)$$

The first of these roots, $A+B$ will always yield the real root, and for this problem, the others are not relevant.

We make the substitutions $p = -\frac{3}{4}$, $q = -\frac{e_{in}}{4}$

to obtain

$$\begin{aligned} e_o &= A+B = \sqrt[3]{\frac{e_{in}}{8} + \frac{1}{8}\sqrt{e_{in}^2 - 1}} + \sqrt[3]{\frac{e_{in}}{8} - \frac{1}{8}\sqrt{e_{in}^2 - 1}} \\ &= \frac{1}{2} \left[\sqrt[3]{e_{in} + \sqrt{e_{in}^2 - 1}} + \frac{1}{2} \sqrt[3]{e_{in} - \sqrt{e_{in}^2 - 1}} \right] \end{aligned} \quad (13)$$

For $e_{in} \geq 1$, it is apparent that e_o is real.

For $e_{in} < 1$, we have $e_{in} - 1 < 0$, so the radicals under the cube roots are pure imaginary. The complex numbers under the cube roots are conjugate to each other, and should be written in the polar form

$$re^{j\theta} \text{ and } re^{-j\theta}$$

$$\text{where } r = \sqrt{e_{in}^2 + |e_{in}^2 - 1|}, \quad \theta = \arctan \left| \frac{e_{in} - 1}{e_{in}} \right|.$$

The cube roots can be obtained by De Moivre's theorem, so

$$e_o = \frac{1}{2} \left[\sqrt[3]{r} e^{j\theta/3} + \sqrt[3]{r} e^{-j\theta/3} \right] \quad (14)$$

The terms in the square brackets are again complex conjugates, so the imaginary part is zero and

$$e_o = \frac{1}{2} \left[2 \sqrt[3]{r} \cos \frac{\theta}{3} \right] \quad (15)$$

because $e^{jA} = \cos A + j \sin A$, $e^{-jA} = \cos A - j \sin A$

so that finally:

$$e_o = \sqrt[3]{r} \cos \frac{\theta}{3}, \text{ which is real} \quad (16)$$

This is too complex for any closed form analytic treatment of complex inputs. Numerical analysis is possible but does not meet the requirements of a general analytic solution.

What we should do now is apply two sine waves as inputs and compute the outputs. This appears feasible only as a point-by-point numerical calculation and is too time consuming to be pursued without greater justification.

2.2.3 Dividers, Bandwidth, and Time - Another Model

a. Heterodyning vs Dividing - When a band of frequencies are heterodyned in a down converter, the bandwidth is preserved. For example, a one mc carrier carrying 5 kc amplitude modulation has 5 kc side bands. When this is mixed with a 900 kc local oscillator, a 100 kc carrier still with ± 5 kc side bands results. Other frequencies result, such as 1900 kc and so on, depending on the circuitry. If the same signal, $1.0 \text{ Mc} + 1.005 \text{ Mc} + 0.995 \text{ Mc}$ is frequency - divided by 10, the resultant frequencies are 100 kc, 100.5 kc and 99.5 kc. The bandwidth has been reduced from 10 kc to 1 kc. An AM modulator would have a 500 cps output.

b. Time Storage - Pursuing this line of reasoning to a lower frequency, consider a 1000 cps wave that slowly varies in amplitude from zero to two volts in a sinusoidal manner. If 10 seconds are required to complete one cycle of the original at the input to a divider, and the frequency division is by two, twenty seconds are required to complete one cycle at the output of the divider.

Continuing to think in terms of time, consider a half-hour TV show arriving on a 60 Mc carrier and use a division ratio of three to pass it through a twenty Mc center frequency IF amplifier. Now the show lasts one and one-half hours. (The picture flickers badly). If we are still watching the show an hour after the show is over, there must be some storage of signal. The storage must accommodate at least 30 minutes of program in this case.

This principle can further be illustrated in the following manner. If a tape recorder is used to record a signal at 30 ips, but the playback is on another tape recorder at 7.5 ips, we have a frequency divider with a divisor of four.

2.2.4 Practical Dividers

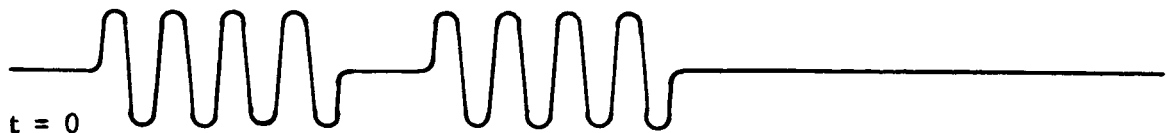
Frequency dividers, as currently conceived and applied, are not true frequency dividers. They servo a signal of lower frequency to one or more parameters of the input signal. Usually the frequency or phase of the incoming signal is the parameter to be followed.

A true frequency divider must have signal storage capability equal in all respects, including period, to the input signal. In the case of the half hour TV show, a storage medium with one and one-half hour capacity was required. This is, of course, true only for a simplified approach to the problem. If the retrace periods are not recorded, the storage capacity requirement is reduced. In the same manner, a radar signal storage requirement may be reduced to, say, a specific interval centered on the expected pulse return time. Such schemes may require switching, delaying, combining and are limited in application. Certainly they are not low-noise receiver front ends.

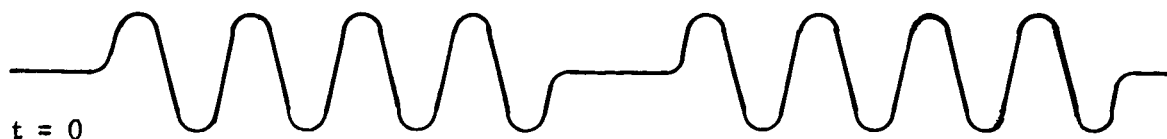
The tape recorder illustration of division can also be applied to frequency multiplication. In division, the tape was played back more slowly than it was recorded, and thus over a longer time. In true multiplication, the tape is played back more rapidly than it was recorded. Then a true multiplier must be able to predict the future to be able to supply the signal faster than it is being received. The closest approach to true multiplication requires storage of the signal for delayed multiplication.

2.2.5 A Carrier Divider

In the preceding section we have discussed a true frequency divider. If it had an input as shown,



divided by 2, the output would resemble



It is recognized that a "carrier divider" is also of great interest. Given the same input and division ratio as in the first example, its output would be



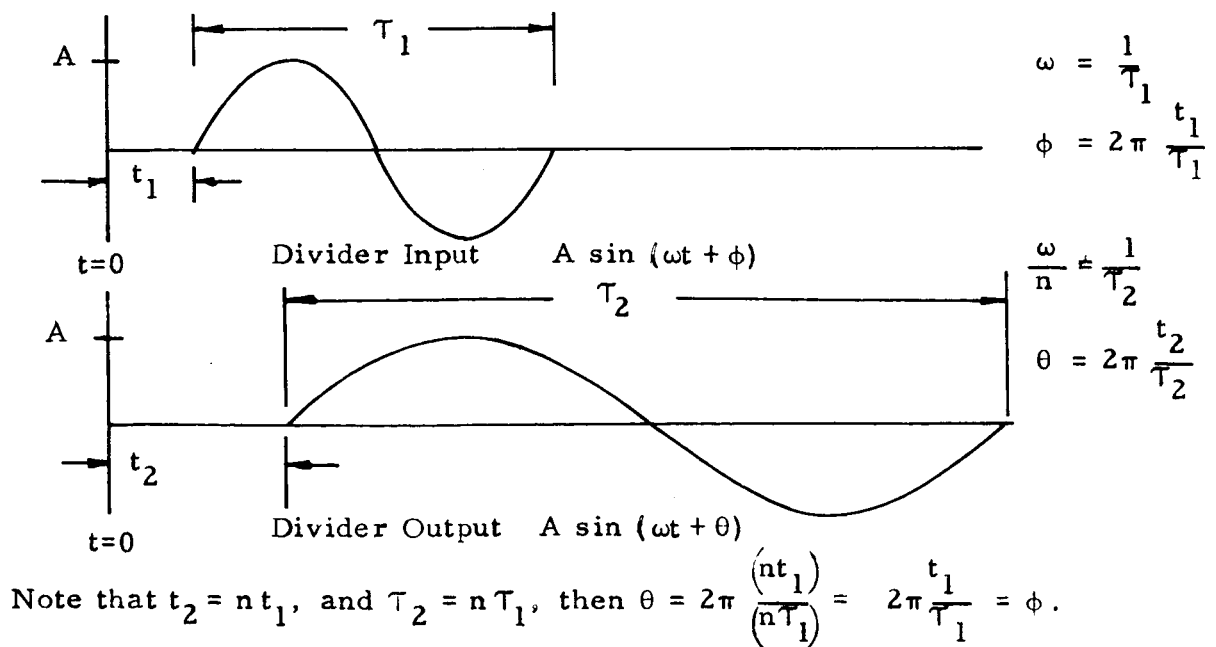
One possible model which would give this action is the step-recovery diode subharmonic generator which will be considered later.

2.3 Effect of Division on Sine and Random Functions

Here the approach used is the calculation of the effect of a divider on random functions applied as inputs. An intermediate conversion of the statistics of the random function is used. The final answer is in terms of the rms value of the function. The relationship of short term phase stability to rms signal-to-noise ratio has been shown in previous work, for example, in SEI letter progress report Dec. 1961, p 26 for Contract No. NAS 8-1643.

2.3.1 The Action of a Frequency Divider Defined

If the input signal is $A \sin \psi = A \sin (\omega t + \phi)$ where A is constant, the desired information is carried on ψ . With this input signal, the output of the assumed frequency divider of ratio n is $A \sin \left(\frac{\omega t}{n} + \theta \right)$. The phase angle θ radians equals ϕ radians, but the time value of θ is n times greater than that of ϕ . This is illustrated below.



2.3.2 The Action of a Divider on a Sine Wave Plus Noise

An incoming signal $y(t)$ is composed of a sine wave plus noise.

$$y(t) = P \cos(\omega_c t + \psi) + x(t). \quad (17)$$

where

P is a constant

ω_c is the sinewave frequency

ψ is uniformly distributed over 0 to 2π . That is, all values of ψ are equally probable between zero and 2π . f_c is $\frac{\omega_c}{2\pi}$ which lies within the band f_1 to f_2 . $x(t)$ is an independent narrow band gaussian process for a band f_1 to f_2 and zero elsewhere. The autocorrelation function of $x(t)$ has exponential decay.

The autocorrelation function of $y(t)$ is

$$R(\tau) = \lim_{T \rightarrow \infty} \frac{1}{2T} \int_{-T}^T y(t) y(t+\tau) dt. \quad (18)$$

If $y(t)$ is rewritten as $s(t) + x(t)$, then

$$y(t) y(t+\tau) = [s(t)+x(t)] [s(t+\tau)+x(t+\tau)] = s(t)s(t+\tau) + s(t)x(t+\tau) + x(t)s(t+\tau) + x(t)x(t+\tau). \quad (19)$$

The autocorrelation function

$$R_y(\tau) = R_x(\tau) + R_s(\tau) + R_{xs}(\tau) + R_{sx}(\tau). \quad (20)$$

The cross-correlation function $R_{xs}(\tau) = \int_{-\infty}^{\infty} G_{xs}(f) e^{j\omega\tau} df. \quad (21)$

where

G_{xs} is the cross-spectral density of $s(t)$ and $x(t)$. However, if two stationary processes are uncorrelated their cross-spectral density is zero at all frequencies. So $G_{xs}(f) = 0$.

Then $R_{xs}(\tau) = \int_{-\infty}^{\infty} [G_{xs}(f) = 0] e^{j\omega\tau} df = 0. \quad (22)$

and $R_{sx}(\tau) = \int_{-\infty}^{\infty} [G_{sx}(f) = 0] e^{j\omega\tau} df = 0. \quad (23)$

This simplifies $R_y(\tau)$ to

$$R_y(\tau) = R_x(\tau) + R_s(\tau) \quad (24)$$

The rms value of $y(t)$ is $\sqrt{R_y(o)}$, and the mean square value of $y(t)$ is $R_y(o)$. $R_y(o) = R_x(o) + R_s(o)$. Then, if $R_x(o)$ and $R_s(o)$ can be evaluated, the rms value of $y(t)$ can be determined.

The rms value of $s(t)$ is the rms value of $P \cos(\omega_c t + \psi)$ which equals $0.707P$. The divided signal $s_n(t) = P \cos \frac{\omega_c t}{n} + \psi$ also has an rms value of $0.707P$. Then the rms value of $s(t)$ is not changed by division. It remains to determine the effect of division on $x(t)$, the random function.

2.3.3 The Action of a Divider On a Band Limited Random Function

A particular random function referred to by many authors ^{1, 2, 3} has an autocorrelation function with exponential decay.

$$R(\tau) = e^{-|\beta\tau|} \quad (25)$$

where β can be considered a constant for this development.

The spectral density of the original function is

$$G(f) = 4 \int_0^{\infty} R(\tau) \cos 2\pi f\tau \, d\tau = \frac{4\beta}{\beta^2 + \omega^2} \quad (26)$$

A frequency divider ($\div n$) would affect $G(f)$, the spectral density, in a predictable fashion

$$G_n(f) = n \left[\frac{4\beta}{\beta^2 + (n\omega)^2} \right] \quad (27)$$

The spectral density consists of two factors. The first, the amplitude factor, represents a frequency independent density increase which is due to packing the original function into small bandwidth. The second, the envelope or shape factor, represents the frequency dependent function of the divided output.

The autocorrelation function of the divided function

$$\begin{aligned} R_n(\tau) &= \int_0^{\infty} G_n(f) \cos 2\pi f\tau \, df \\ &= \int_0^{\infty} \frac{4n\beta}{\beta^2 + (n2\pi f)^2} \cos 2\pi f\tau \, df \end{aligned} \quad (28)$$

Because of the form of this function, it is not integrable.

Since the change in rms value of the function is the value desired, and since we have noted $\sqrt{R_y(o)}$ = rms value of $y(t)$ earlier, we will evaluate $R(o)$ and $R_n(o)$ for comparisons. We also want to introduce the band limited

restrictions for both input and output here. That is, the spectral density of the original function is zero outside the band f_1 to f_2 , and the divided function is zero outside the band $\frac{f_1}{n}$ to $\frac{f_2}{n}$.

$$R(o) = \int_{f_1}^{f_2} \frac{4\beta}{\beta^2 + \omega^2} \cos 2\pi f (T=0) df$$

$$= \int_{f_1}^{f_2} \frac{4\beta}{\beta^2 + \omega^2} df \quad (29)$$

$$= \frac{2}{\pi} \left[\tan^{-1} \frac{2\pi f_2}{\beta} - \tan^{-1} \frac{2\pi f_1}{\beta} \right] \quad (30)$$

$$R_n(o) = \int_{f_1/n}^{f_2/n} \frac{4n\beta}{\beta^2 + (n\omega)^2} df \quad (31)$$

(note the integral is over the new bandwidth)

$$R_n(o) = [4n] \left[\frac{1}{2\pi n} \right] \left[\tan^{-1} \frac{2\pi f n}{\beta} \right]_{f_1/n}^{f_2/n}$$

$$= \frac{2n}{n\pi} \left[\tan^{-1} \frac{2\pi f_2}{\beta} - \tan^{-1} \frac{2\pi f_1}{\beta} \right]$$

$$= \frac{2}{\pi} \left[\tan^{-1} \frac{2\pi f_2}{\beta} - \tan^{-1} \frac{2\pi f_1}{\beta} \right] \quad (32)$$

The ratio of the rms value of the divided function to the rms value of the original is

$$\frac{\sqrt{R_n(o)}}{\sqrt{R(o)}} = \sqrt{\frac{\tan^{-1} \frac{2\pi f_2}{\beta} - \tan^{-1} \frac{2\pi f_1}{\beta}}{\tan^{-1} \frac{2\pi f_2}{\beta} - \tan^{-1} \frac{2\pi f_1}{\beta}}} = 1 \quad (33)$$

2.3.4 Effect of Divider on Spectra

The divider, as we have previously defined it, has no "discrete frequency" power gain. The signal power output at a single frequency equals the signal power input at n times that frequency. We want to see what this means in terms of continuous spectra.

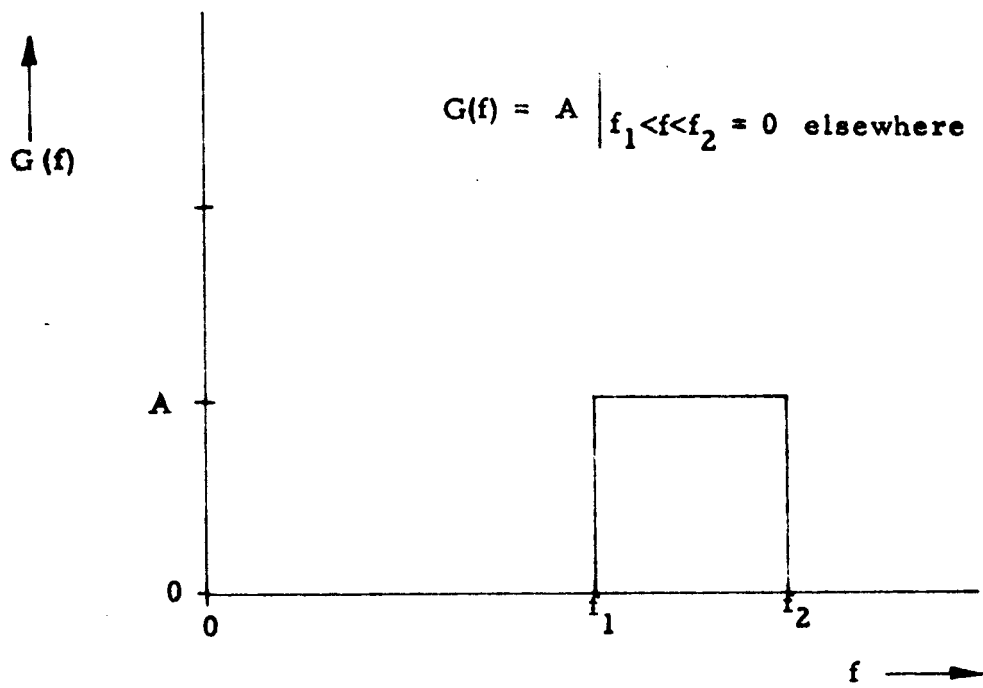
For band limited white noise, the spectral density is as shown in Fig. 3 (a). If this function is the input of a divider, the spectral density of the divider will be shown in Fig. 3 (b).

For an arbitrary spectral density shown in Fig. 4 (a), the effect of the divider is shown in the spectral density of the output shown in Fig. 4 (b).

A third example uses the interesting servo-noise function characterized as having an exponentially decaying autocorrelation function. Elsewhere in this report we have derived the spectral density as $G(f) = \frac{4\beta}{\beta^2 + \omega^2}$. For $\beta = 1$, and a further limitation that $G(f) = 0 \mid_{\omega > 6}$. The spectral density of the original function is shown in Fig. 5 (a).

Though the rms values of divided functions are not reduced the length of time or duration of the function is increased by n , thus the "energy"* of the function is increased by a divider. The third example is shown again with the time axis included in Fig. 6.

* Energy is a valid concept when the functions have the dimensions of voltage or current and time.



(a) Band Limited White Noise at the Divider Input

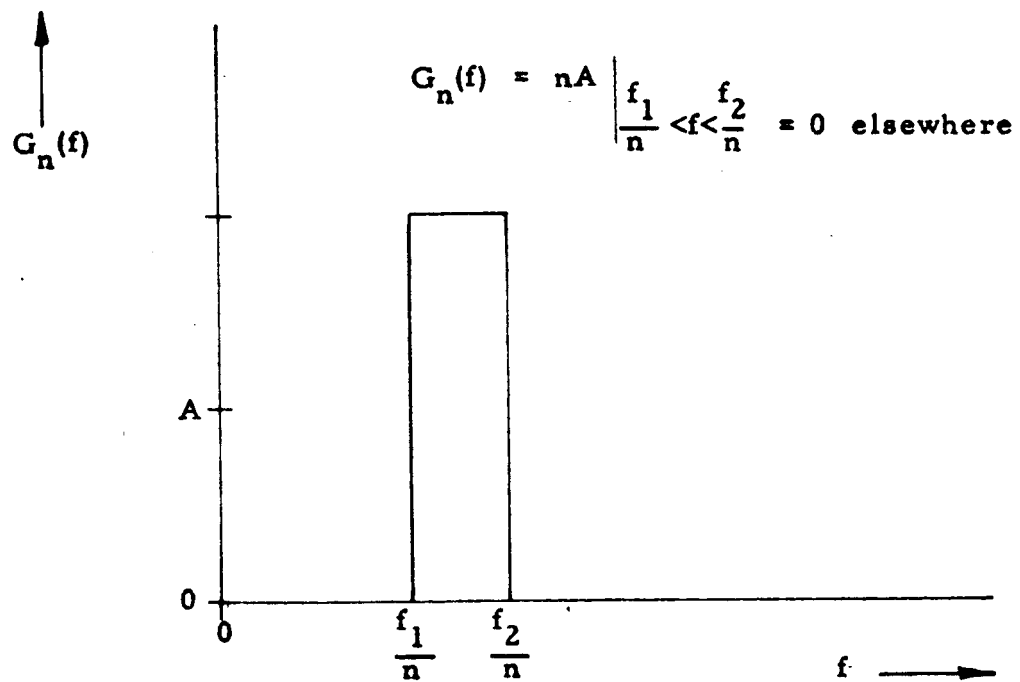
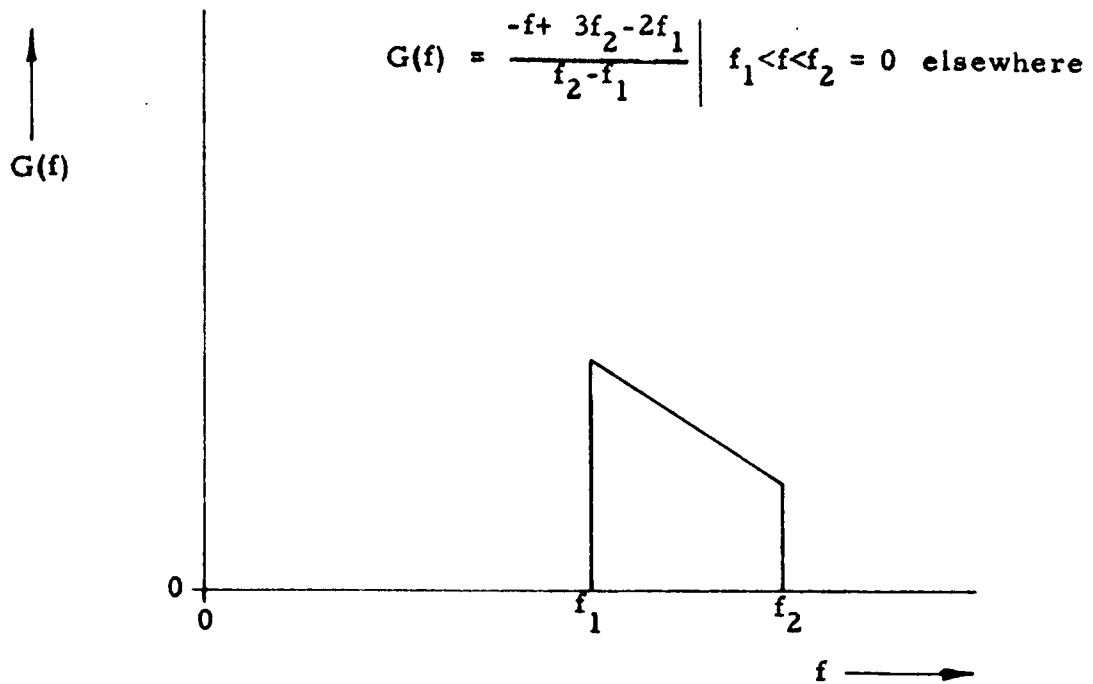
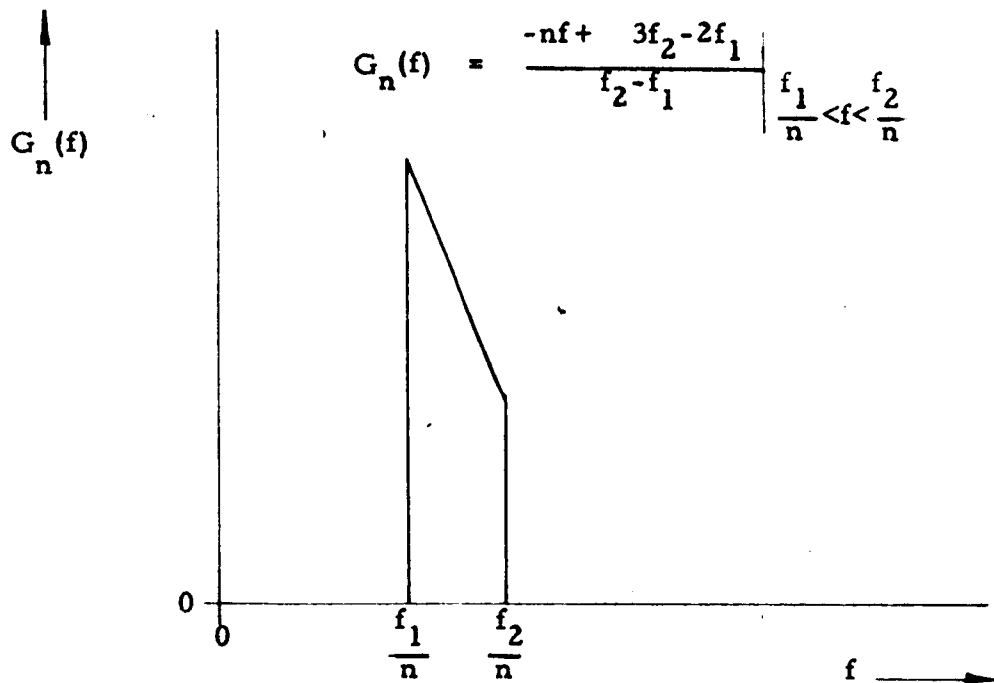
(b) Band Limited White Noise After Division by n

FIG. 3 THE EFFECT OF A DIVIDER ON WHITE NOISE





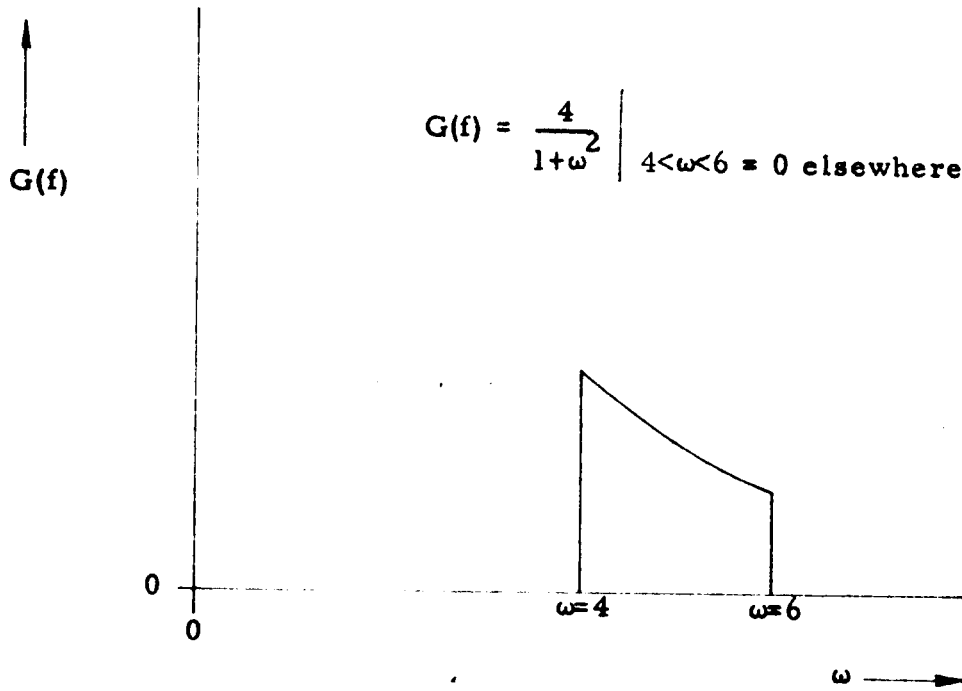
(a) Spectral Density of an Arbitrary Function



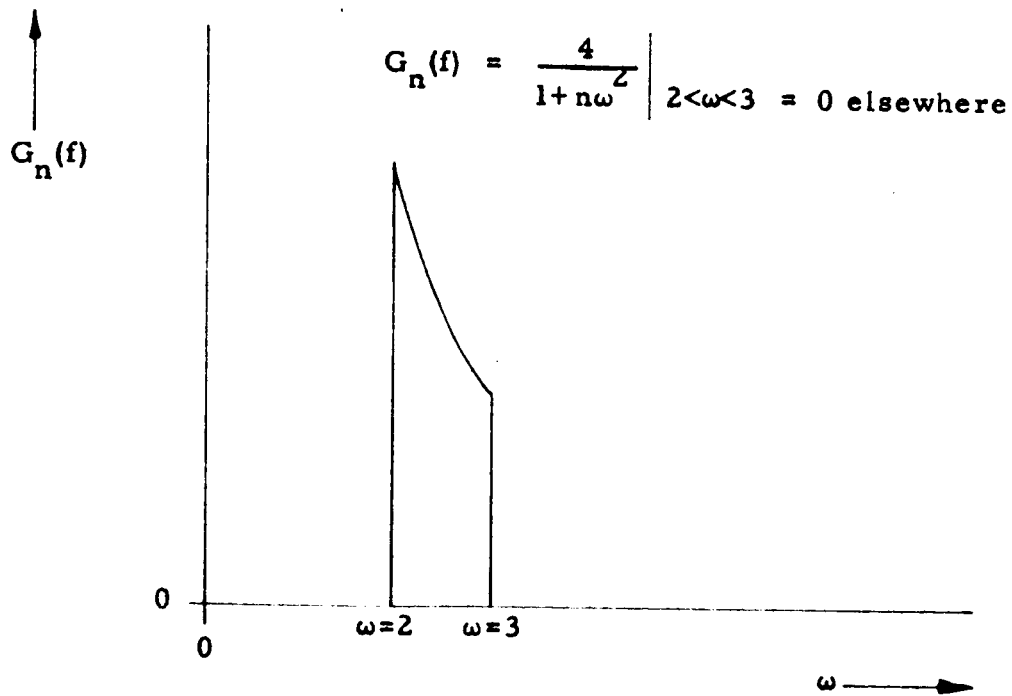
(b) Spectral Density of the Divided Function

FIG. 4 THE EFFECT OF A DIVIDER ON THE SPECTRAL DENSITY OF AN ARBITRARY FUNCTION





(a) Spectral Density of the Input Function



(b) Spectral Density of the Divided Function



FIG. 5 THE EFFECT OF A DIVIDER ON A SERVO
AND COMMUNICATIONS RANDOM FUNCTION

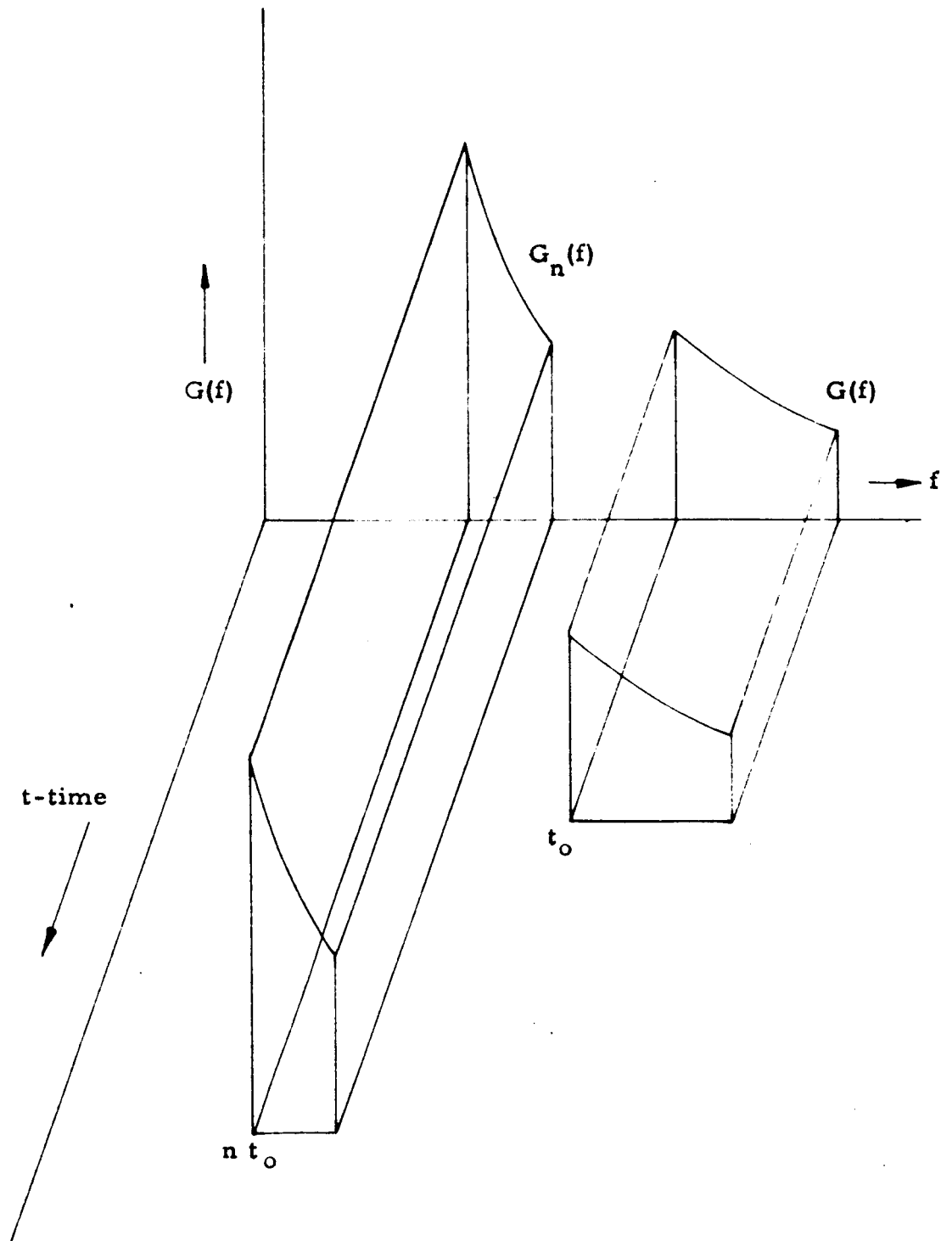


FIG. 6 THE EFFECT OF A DIVIDER ON THE SPECTRAL DENSITY OF THE RANDOM FUNCTION OF FIG. 5



2.3.5 Conclusions

a. There is no change in the rms value of any functions studied to date as a direct result of simple frequency division. This is true so long as the periods of observation of the original and divided signal are the same and equal, or exceed the time required to fulfill the conditions of a stationary process.

b. The duration of the signal out of a divider is greater than the duration of the input by a factor n , the division ratio. Then, if rms signal represents power, the output energy is n times the input energy and there must be an energy input to the divider.

2.4 Application of Step-Recovery Diode to Division

Subharmonic generators were considered as representing the simplest class of frequency divider having the output locked to a parameter of the input. The theory of non-linear reactance subharmonic generation was reviewed and some experimentation conducted with varactors in this application. This led to experimental use of the step-recovery (charge-storage, snap-off, Boff) diode on the assumption that its high efficiency harmonic generation might be due to a mechanism which could also generate subharmonics.

After successfully achieving subharmonic generation with the step-recovery diode, a theoretical understanding was sought in terms of certain postulated models.

2.4.1 Manley-Rowe Frequency - Power Relation

If the step-recovery diode can be considered a time-varying capacitor, its performance should be predictable by the Manley-Rowe⁴ relation. For a lossless reactance in a tuned network with power flow restricted to frequencies ω_1 , ω_2 and $\omega_3 = \omega_1 - \omega_2$, the Manley-Rowe formulas reduce to

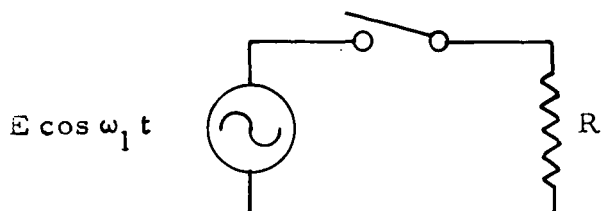
$$\frac{P_2}{\omega_2} = \frac{P_3}{\omega_3} = -\frac{P_1}{\omega_1} \quad (34)$$

Therefore, the maximum efficiency of a subharmonic generator obeying this law would be given by the ratio of output to input frequencies.

For example, in the case when the input frequency is 13 times the output, the maximum efficiency would be 7.57% and, for a lossless component, the remaining power must be dissipated in the idler (ω_2) circuit.

2.4.2 Switch Energy - Power Relation

An interesting lossless device which does not obey the Manley-Rowe formulas is the switching circuit derived by Penfield⁵. The circuit is shown below.



The switch is open half its period $T_2 = \frac{2\pi}{\omega_2}$.

Assuming $\omega_2 = 12\omega_1$ for an up-conversion case

$$P_1 = \frac{E^2}{8R} \quad (\text{at } \omega_1) \quad (35)$$

$$P_3 = \frac{E^2}{2n^2 \pi^2 R} \quad (n \text{ odd}) \quad (36)$$

for all output frequencies $\omega_3 = n\omega_2 \pm \omega_1$.

Then, if $\omega_3 = 13\omega_1$, and $n = 1$, and if power is permitted to flow at only the three frequencies of interest, the efficiency is $4/\pi^2 \approx 40.5\%$.

This analysis does not apply to dividers. However, it is possible to use a similar approach for the divider case.

2.4.3 Quantum Mechanical Basis for Energy-Power Formulas

The three frequency converter has been shown by Weiss⁶ in a quantum mechanical derivation to obey energy-power relations identical to those based on the Manley-Rowe equations. The analysis is based on the conservation of quanta and the emission or absorption of radiation accompanying the transition between energy states. It is true for any energy-state system.

2.4.4 Mechanism of Subharmonic Generation

The generation of negative resistance in junction diodes has been observed by experimenters^{7,8} and has been attributed to two mechanisms: RF induced and that due to minority carrier storage.

a. RF induced negative resistance can exist whenever the diode is coupled to a circuit resonant at the driving frequency and when the non-linear diode capacitance is appreciable compared to any linear capacitance in the circuit. In experimental work, this mechanism would be indicated by the requirement for a resonant circuit at the driving frequency.

b. Minority carrier negative resistance does not require a resonant circuit at the driving frequency. The only requirement is that the period of driving signal not be appreciably longer than the minority carrier lifetime. Further experimental work may lead to identification of the mechanism involved in subharmonic generation with diodes, and step-recovery diodes in particular.

2.4.5 Experimental Subharmonic Generation

The first experimental subharmonic generator constructed and tested utilized a varactor as the non-linear element and produced an output at 1/4 the input frequency. It was observed that a high input level was necessary in order to generate an output with any stability.

Prior to attempting to use the step-recovery diode in this application, some experimental verification of the claims made for this type of diode as a harmonic generator was undertaken. In general, it was found that the step-recovery diode is indeed capable of high-order high-efficiency frequency multiplication and without needing resonant idler circuits. A typical result obtained experimentally was a X5 circuit which yielded 17 mw at 2280 Mc from an input of 100 mw at 456 Mc. This operation was not regarded as optimum, but rather as an indication of the potential of the device.

The $\div 4$ subharmonic generator was tested with an SSA550 snap-off diode. 1 mw at 2280 Mc input resulted in a stable locked output at 570 Mc of .18 mw. This circuit utilized an idler at 1140 Mc. The performance of this circuit with the snap-off diode (essentially a step-recovery

diode) was a marked improvement with respect to lower drive level, efficiency and stability as compared with the same circuit using a varactor.

A $\div 13$ subharmonic generator was fabricated and tested. In this case, it was elected to use the three-frequency conversion approach described by Manley and Rowe as the inverting demodulator case, with an idler at 12 times the output frequency. When properly tuned and matched, a stable locked output of 1.8 mw at 175 Mc with an input of 30 mw at 2280 Mc, or 6% efficiency, was obtained.

Figure 7 indicates the frequencies at which various circuit components operate. A simple matching network is used at the input. It will be noted that the diode is coupled directly to the input resonator by using it as a loop adjacent to the center conductor of the resonator. A trap at the input frequency follows. The idler circuit operates at $\frac{n-1}{n} f$ where n is the division factor and f is the input frequency. The remainder of the circuitry resonates, controls phase and matches the input frequency. A simpler output matching network might possibly be used; however, it is felt that the extra degrees of freedom provided by the network employed makes it almost essential at least during tuneup. Both SSA550 snap-off diodes and hpa 0153 step-recovery diodes seemed to perform adequately in this circuit.

The circuit shown is not easily tuned, since frequency-locked subharmonic oscillation can only occur when all adjustments are nearly optimized. The procedure followed at SEI follows:

- a. The tuneup uses a spectrum analyzer for output indication along with a low-pass (195 Mc cut-off) filter to eliminate spurious responses.
- b. Initially the output network is grid-dipped at about 175 Mc and the trap and idler circuits set at minimum capacitance.
- c. With a 2280 Mc signal of about 100 mw level, the input resonator is tuned for maximum 2280 Mc output at the 175 Mc terminal (LP filter removed). The trap is then adjusted to minimize this 2280 Mc output.
- e. With 2280 Mc input and maximum sensitivity of the spectrum analyzer at 175 Mc, the idler and matching capacitors are rocked for

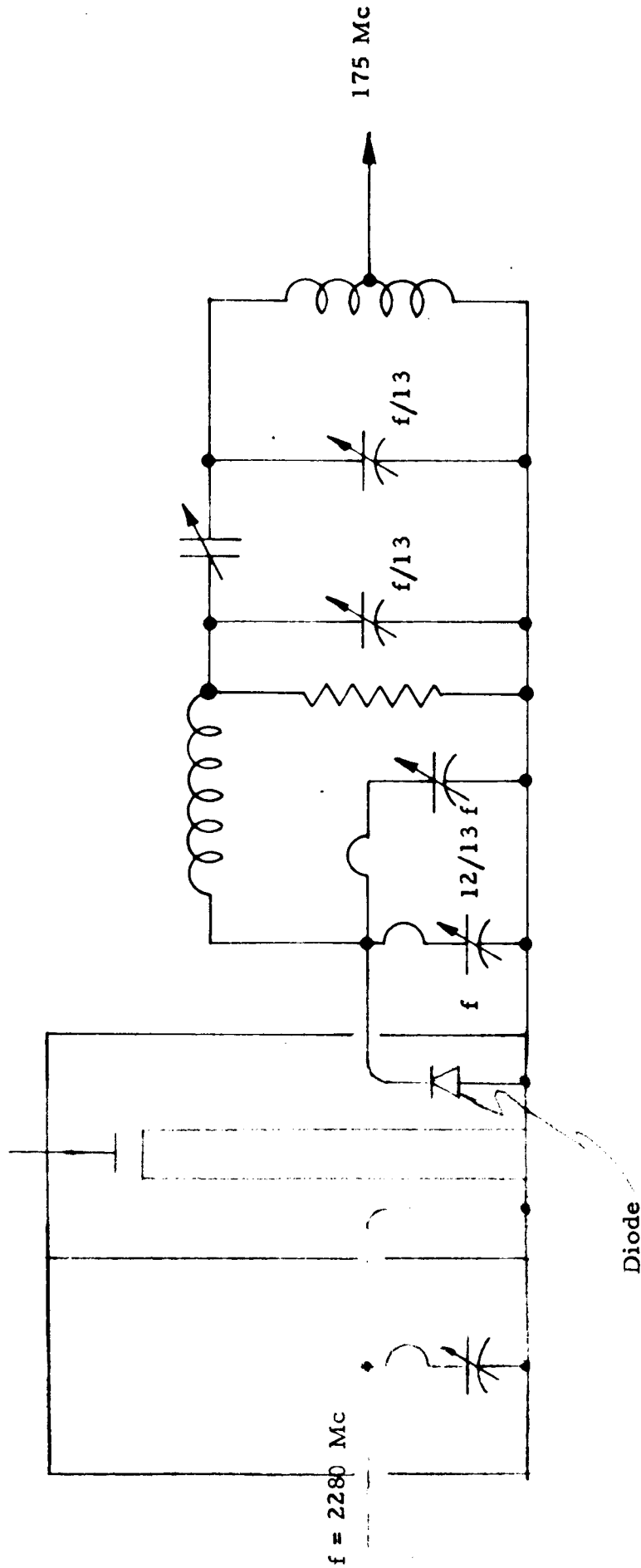


FIG. 7 SCHEMATIC OF REVISED $\div 13$ SUBHARMONIC GENERATOR



maximum noise output at 175 Mc. Proper adjustment will produce an abrupt rise in this noise. Continued adjustment will eventually produce a free oscillation at about 175 Mc, and this will jump into lock when conditions are near optimum. From this point, fine tune-up for maximum efficiency is similar to multiplier tuneup.

f. Continuous monitoring of input matching during tuning is found to be helpful. This can be done by using 2280 Mc 3db hybrid or circulator to isolate forward and reflected power. The reflected power can be monitored with an RF power meter.

Certain observations regarding tuneup and testing may be in order. The low pass filter is essential, at least with a spectrum-analyzer, to avoid tuning up on spurious responses, since the charge-storage diode is an excellent harmonic generator.

When tuneup is completed, the output frequency is definitely locked to the input frequency, with variation of input frequency producing a corresponding output frequency change.

Measurement of efficiency must be done with care. The input must be well matched with most methods of power measurement. Also the presence of spurious output frequencies makes a broadband RF wattmeter measurement of the 175 Mc output unreliable. The method used at SEI in checking output power is substitution, i.e. the spectrum analyzer is used as an indicator, and a clean source of 175 Mc substituted for the divider into the 50 ohm load, and its level adjusted to give the same indication as the divider. Then the output of the signal source is measured with a 50 ohm hp power meter. Care must be taken again to ensure that the load used for both divider and substitute source is truly 50 ohms.

Two \div 13 units were constructed using the layout of Fig. 8 and very nearly identical results were achieved. The two units were operated from a common source of 2280 Mc power and their outputs combined with suitable isolation into a spectrum analyzer. The resulting display showed a single response the height of which could be varied by adjusting the phase delay of one of the 175 Mc outputs with a line stretcher. Moreover, the outputs of the two units varied identically in frequency as the common input frequency was varied.

309A

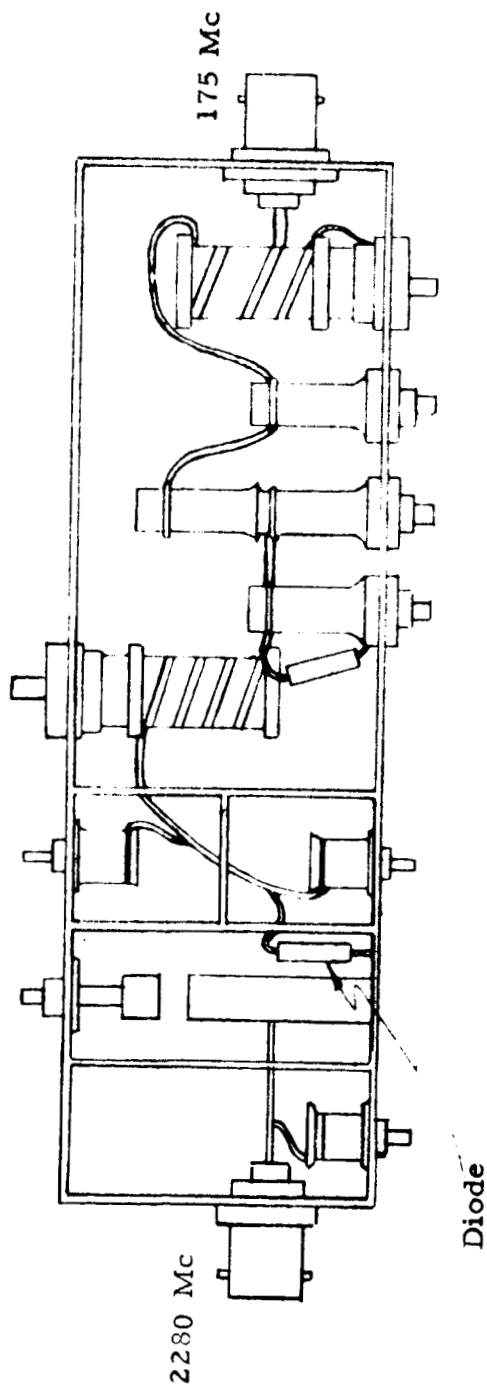


FIG. 8 ÷ 13 SUBHARMONIC GENERATOR USING CHARGE-STORAGE DIODE



A further check of frequency locking was conducted by frequency modulating the input frequency to the divider and observing the output. The modulated 2280 Mc input frequency was obtained by use of a frequency-modulated 143 Mc source at 10 watts followed by a X16 varactor multiplier having 1.1 watts output at 2280 Mc. With suitable attenuation and band-pass filtering, this signal was used as the input to one of the $\div 13$ units. Figure 9 shows the modulated output of the 143 Mc source in a) and the 175 Mc output of the divider in b). A block diagram of the setup appears in Fig. 10.

Phase stability was measured using the two $\div 13$ units in the setup of Fig. 11 and using the procedure described in NAS 8-1643 report dated March 1963. The measured value of phase jitter was 0.028 degrees per divider, or 5×10^{-4} rad.

3. RF AMPLIFIER PROGRAM

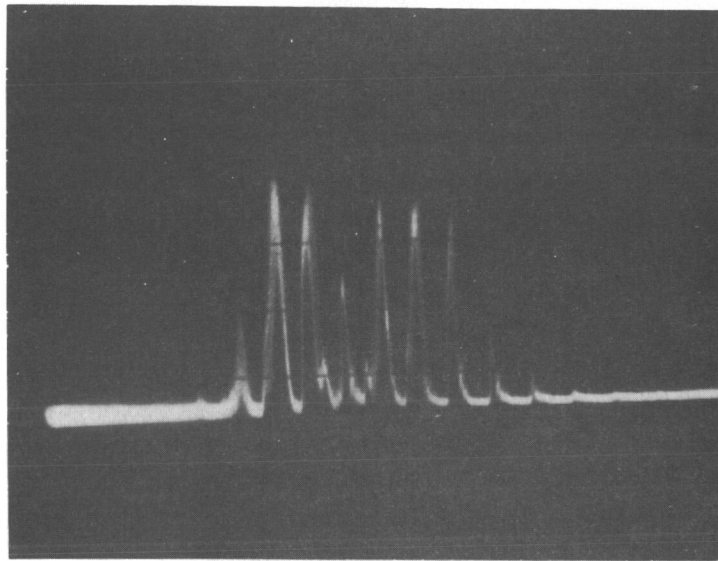
The problem of handling a low-level received signal with minimum degradation of signal-to-noise ratio was attacked by two approaches: low-noise parametric amplification and tunnel-diode down-conversion with gain. A study of the various types of paramps was conducted with some experimental verification of theory using the S-band breadboard paramp constructed during Contract NAS 8-1643. Most of the tunnel-diode down-converter work was experimental and was conducted at both L- and S-band frequencies.

3.1 Parametric Amplifier Study

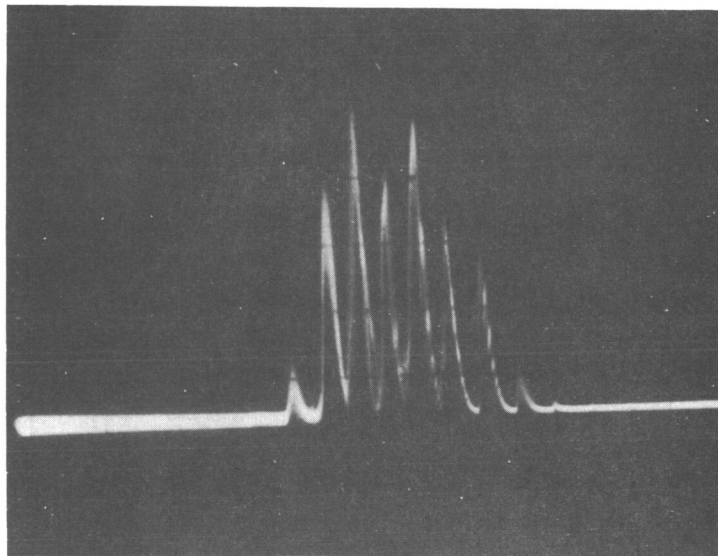
3.1.1 Description of Types

There are two principal types of parametric amplifiers: the up-converter and the negative-resistance amplifier. The up-converter is pumped at a frequency higher than the signal and the output frequency is the sum of the signal and pump frequencies. Its maximum theoretical gain, as predicted by the Manley-Rowe power relations for non-linear lossless reactances is given by the ratio of output to input frequencies.

The negative-resistance amplifier, on the other hand, has identical signal input and output frequencies and depends on the generation of a negative resistance at the signal frequency for amplification. It will have



a. 143 Mc INPUT TO CHAIN



b. 175 Mc OUTPUT OF
SUBHARMONIC GENERATOR

FIG. 9 SPECTRUM DISPLAY OF MODULATED CARRIER

(See Fig. 10)



312A

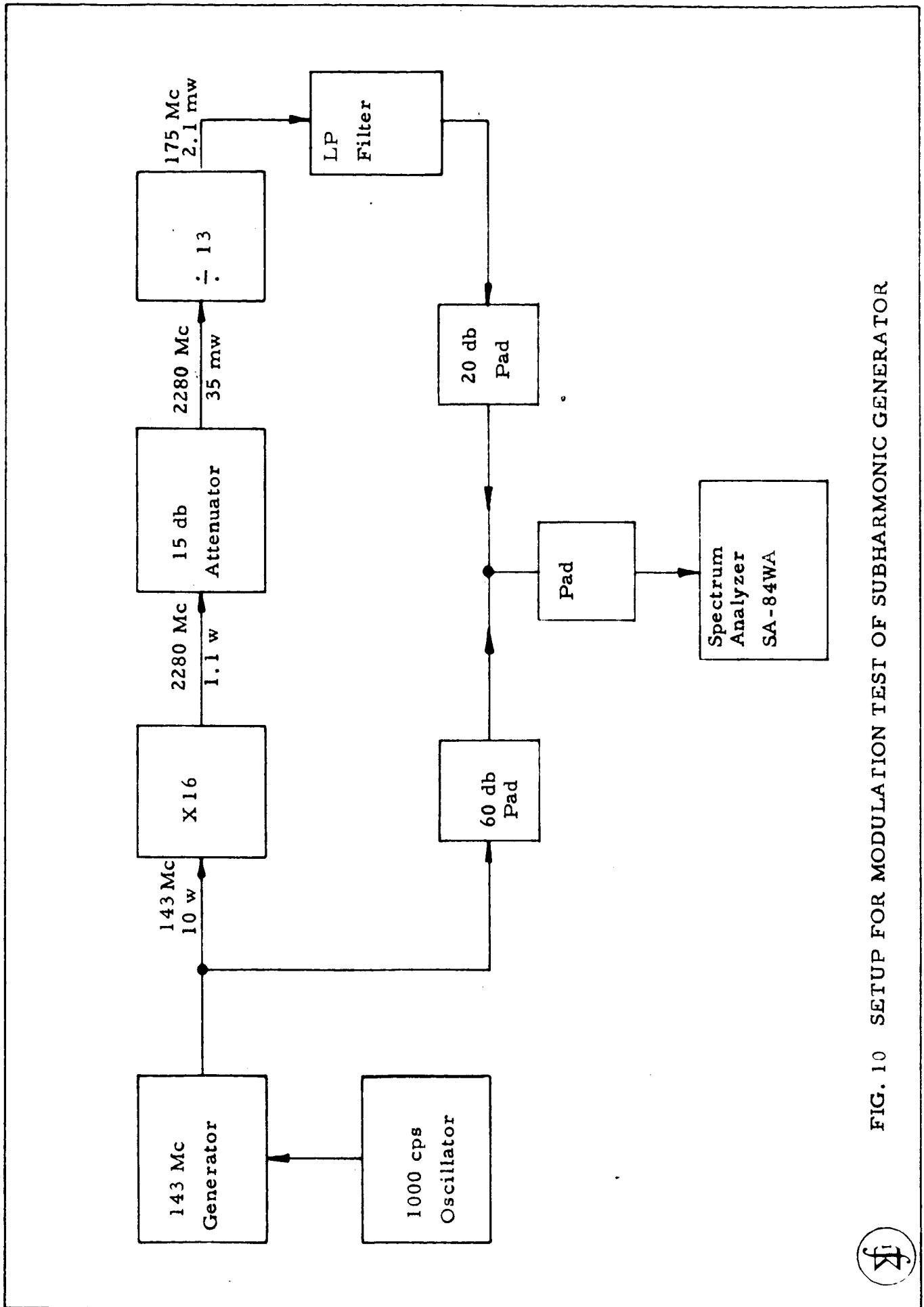


FIG. 10 SETUP FOR MODULATION TEST OF SUBHARMONIC GENERATOR



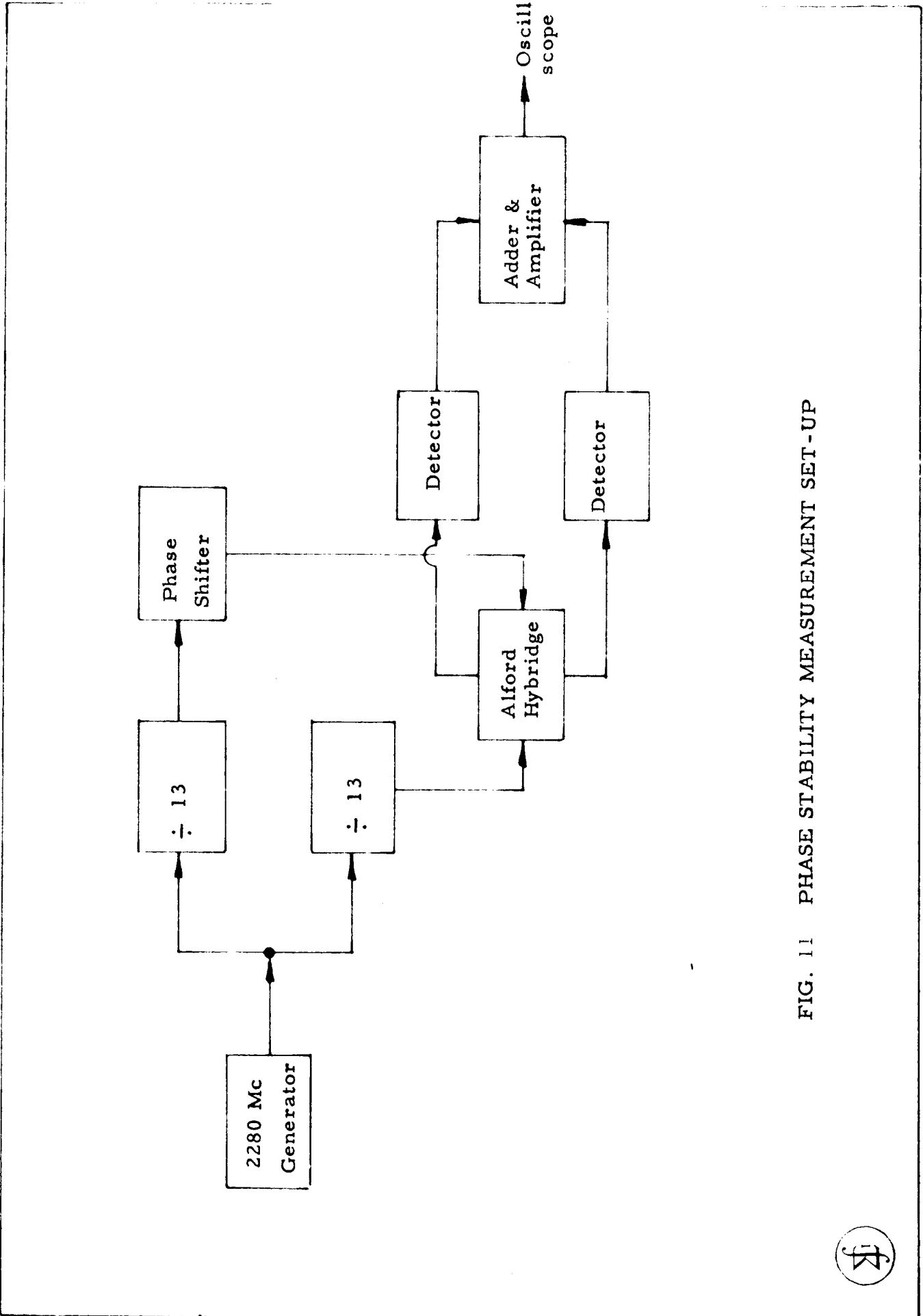


FIG. 11 PHASE STABILITY MEASUREMENT SET-UP



power flowing at signal and pump frequencies and at one or more idler frequencies.

Moreover, there are two principal types of negative resistance amplifier. The non-degenerate amplifier is ordinarily pumped at a frequency several times that of the signal and has an idler at the difference frequency. The degenerate amplifier has both signal and idler frequencies within the same pass-band which requires a pump frequency of approximately twice the signal frequency. A special case would be that of the "phase-coherent" degenerate amplifier where the signal and idler are at identical frequencies.

Typically, the negative-resistance amplifier is a single-port device with respect to the signal. The negative resistance generated at the parametric element results in greater reflected than incident power. Usually a circulator is used to separate the reflected from the incident power and thus provide input and output signal ports with positive impedances.

Special types of negative-resistance paramps employing more than one idler can operate without circulators and at the same time are capable of operation at pump frequencies less than the signal.

3.1.2 Characteristics

In the usual communications applications the optimum noise figures of the conventional paramp types discussed above are identical. In other respects, their characteristics vary greatly.

a. Upconverter - This is a unilateral, stable device with greater bandwidth than the negative resistance amplifier. The gain obtainable is rather limited, since it is dependent on the ratio of output to input frequencies.

A further problem is that most applications require subsequent down-conversion which is difficult to achieve with good noise figure if the output frequency of the upconverter is very high. This makes the use of the upconverter questionable at signal frequencies greater than 1000 Mc.

b. Negative Resistance Amplifier - Many of the characteristics of the negative resistance parametric amplifier result from the use of a circulator. The circulator contributes stability, noise figure improvement and unilateral gain. On the other hand, the circulator increases the size, weight and complexity of the amplifier. It adds insertion loss and may

restrict the bandwidth unduly unless its own bandwidth is adequate.

The negative resistance amplifier achieves maximum gain on the verge of oscillation. Therefore, its maximum gain is limited principally by stability considerations.

The high pump frequency of the usual non-degenerate amplifier causes the idler frequency to fall outside the signal passband, resulting in single-side-band operation, a desirable condition in communication applications. However, the high frequency pump has its disadvantages, since pump stability is closely related to gain stability.

The degenerate type amplifier has a lower pump frequency (approximately twice the signal frequency). Idler power appears in the signal passband, and if the application permits this type of operation, the resulting double side-band noise figure will be better than the SSB noise figure of the corresponding non-degenerate amplifier. Moreover, reduction of cavity loss at the lower idler frequency with respect to diode loss can further enhance the noise figure.

When the presence of the idler frequency in the signal passband is intolerable, a balanced arrangement of two identical degenerate amplifiers can be used to eliminate the idler in the output.

"Phase coherent" operation of the degenerate amplifier requires that the pump be at exactly twice the signal frequency at all times, which is difficult to achieve, especially if the signal frequency has possibility of slight variation.

Table 1 gives the theoretical optimum performance for the conventional types of paramp. The symbols used are defined as follows:

T_a	=	Antenna temperature, degrees Kelvin
T_d	=	Diode temperature, degrees Kelvin
γ	=	Capacitance change coefficient, typically 0.3
Q	=	Diode Q at signal frequency
γQ	=	Figure of merit
b	=	Fractional bandwidth
Q_1	=	Loaded circuit Q at signal input frequency
g	=	Transducer power gain
ω_1	=	Signal input frequency, rad/sec.
ω_2	=	Idler frequency, rad/sec.
ω_3	=	Pump frequency, rad/sec.
ω_4	=	Up-converter output frequency, rad/sec.

TABLE 1

COMPARISON OF CONVENTIONAL TYPES OF PARAMETRIC AMPLIFIERS

	<u>Up-Conversion</u>	<u>Neg. -Res. Amp. with Circ</u>	<u>Degen. Amp. with Circ.</u>
Minimum Operating Noise Temp.	$2 T_d \left[\frac{1}{\gamma Q} + \frac{1}{(\gamma Q)^2} \right] + T_a$	$2 T_d \left[\frac{1}{\gamma Q} + \frac{1}{(\gamma Q)^2} \right] + T_a$	$T_d \left[\frac{1}{\gamma Q} + \frac{1}{(\gamma Q)^2} \right] + T_a$ *
Max. Gain	$\frac{1}{4} (\gamma Q)^2$	∞	∞
Max. Fractional Bandwidth Single Tuned Circuits	$b = \frac{2}{Q_1} \leq 2\sqrt{\omega_4/\omega_1}$	$b = g^{-1/2} \sqrt{\omega_2/\omega_1}$	$b = g^{-1/2} \gamma$
Optimum Pump Frequency for min. Noise Freq.		$\omega_3 = \omega_1 \sqrt{1 + (\gamma Q)^2}$	$2\omega_1$

From Kotzebue, K.L., and L.A. Blackwell, "Semi-conductor- Diode Parametric Amplifiers", Prentice-Hall, Inc., Englewood Cliffs, N.J. 1961

* dsb

3.1.3 Stability Considerations

With the negative-resistance amplifier stability is a serious problem not only to satisfy application requirements but to prevent oscillation. With the paramp operated close to oscillation for high gain, small changes in impedance or pump levels could cause oscillation.

When a circulator is used for separating the input and output signals, insufficient isolation can produce regeneration. The circulator isolation should be 10 db greater than the amplifier gain for good stability. Cascaded stages may be used for greater gain.

Small variations in the total series resistance at the signal frequency can result in quite large gain changes. VSWR stability of the circulator should be held to better than ± 0.5 db. Variation in the negative resistance generated also affects gain. The latter effect can result from pump level instability. 0.1 db change in the power absorbed by the diode can result in 1 db change in gain.

Pump power level changes alter the average capacitance of the diode, producing detuning. Pump frequency variation results in shift of the idler frequency with similar results. Detuning by average capacitance change will also result from bias variation. Furthermore, varying the bias, changes the amount of power absorbed by the diode.

Gain variations can also be caused by unwanted propagation of the idler frequency into the signal circuit. This causes reflections because the signal circuit is not designed to terminate the idler frequency. These reflections distort the idler passband and a corresponding signal passband discontinuity will occur. Solution, install Lo pass filter in signal circuit.

Care should also be taken so that the idler does not propagate in the pump waveguide by having the idler frequency below the cutoff frequency of the pump waveguide.

It is apparent that stability is affected by many factors, and the effects are often interlocking. The principal problem areas appear to be pump and impedance stability. With careful control of pump frequency, and by broadbanding, and the use of pump levelling or limiting, gain stabilities of ± 0.5 db per day and 0.1 db per hour are attainable. The use of high

quality circulators and possibly isolators to stabilize signal impedances will contribute substantially to gain stabilization and control of oscillation.

Most of the factors that determine long-term gain stability such as circulators, pump sources, pump attenuators, the junction capacitance of the diode, etc. are temperature sensitive. Controlled environment is therefore indicated for best stability.

3.1.4 Choice of Type of Parametric Amplifier

The selection of a paramp for a specific application requires detailed knowledge of the system requirements. The following considerations will determine to a large extent the type of paramp to be used in a given situation.

- a) Frequency of input signal.
- b) Frequency stability of input signal at its source.
- c) Bandwidth of signal.
- d) Type of modulation.
- e) Anticipated signal strength or dynamic range.
- f) Signal source impedance variation.
- g) Source signal-to-noise ratio and its stability.
- h) Output signal-to-noise ratio requirement.
- i) Gain required.

At frequencies up to X-band, the most likely choice will be the non-degenerate negative-resistance amplifier. The degenerate type, however, because of its relative simplicity and low pump frequency, should be seriously considered. The lower pump frequency lends itself to a solid state pump with its possibility of good frequency and level stability. However, the rapid progress in the state-of-the-art in solid-state power generation at high frequencies, could minimize this advantage.

Multiple-idler amplifiers with low frequency pumping are a strong possibility at millimeter wavelengths.

An approach to be kept in mind is the possibility of using cascaded, balanced, or hybrid arrangements. The latter approach can be used to combine the advantages of two types for overall system improvement.

An illustration would be the use of an upconverter followed by a degenerate amplifier. Most of the gain would be provided by the degenerate amplifier, while the upconverter would serve as an isolator with gain. The degenerate amplifier would, of course, have to be followed by a down-converting mixer in the typical communication application, but rapid progress in low noise microwave diodes, including hot-carrier diodes, make this less of a problem than previously.

Such a hybrid arrangement offers low overall noise figure, reasonable gain, and low sensitivity to changes in source impedance.

3.2 Tunnel Diode Down-Conversion

Since a number of investigators have indicated that the tunnel diode is capable of operation as a low noise mixer with gain, an experimental program was conducted, directed toward evaluating various TD down converter circuit arrangements as a substitute for the more conventional approach of an RF amplifier and resistive mixer. While the results were inconclusive, and the approach abandoned, the program did provide useful circuit configurations and a better knowledge of the difficulties involved in the application of tunnel diodes.

Work was done at frequencies in L- and S-band; the former because of possible application to a radar altimeter problem, and the latter because of the availability of certain components. The IF frequency was 60 Mc.

3.2.1 Balanced Micro-strip Design

Initial experimentation was carried out with a balanced mixer similar to the unit constructed by SEI during Contract NAS 8-1643. The circuit is shown in Fig. 12 and consists of 1610 Mc signal input matching stubs, unbalanced to balanced transformer and 60 Mc IF matching network. The device proved to be impractical because of difficult and unreliable tuning and because of its bulk.

3.2.2 Balanced Coaxial Hybrid Design

Figure 13 shows a balanced downconverter using a coaxial hybrid ring to obtain balanced signal input at 1610 Mc and to provide isolation between the local oscillator and signal inputs. The hybrid was constructed with RG 187/U 75 Ω miniature coaxial cable. The IF transformer primary was split so as to permit separate biasing of the tunnel diodes.

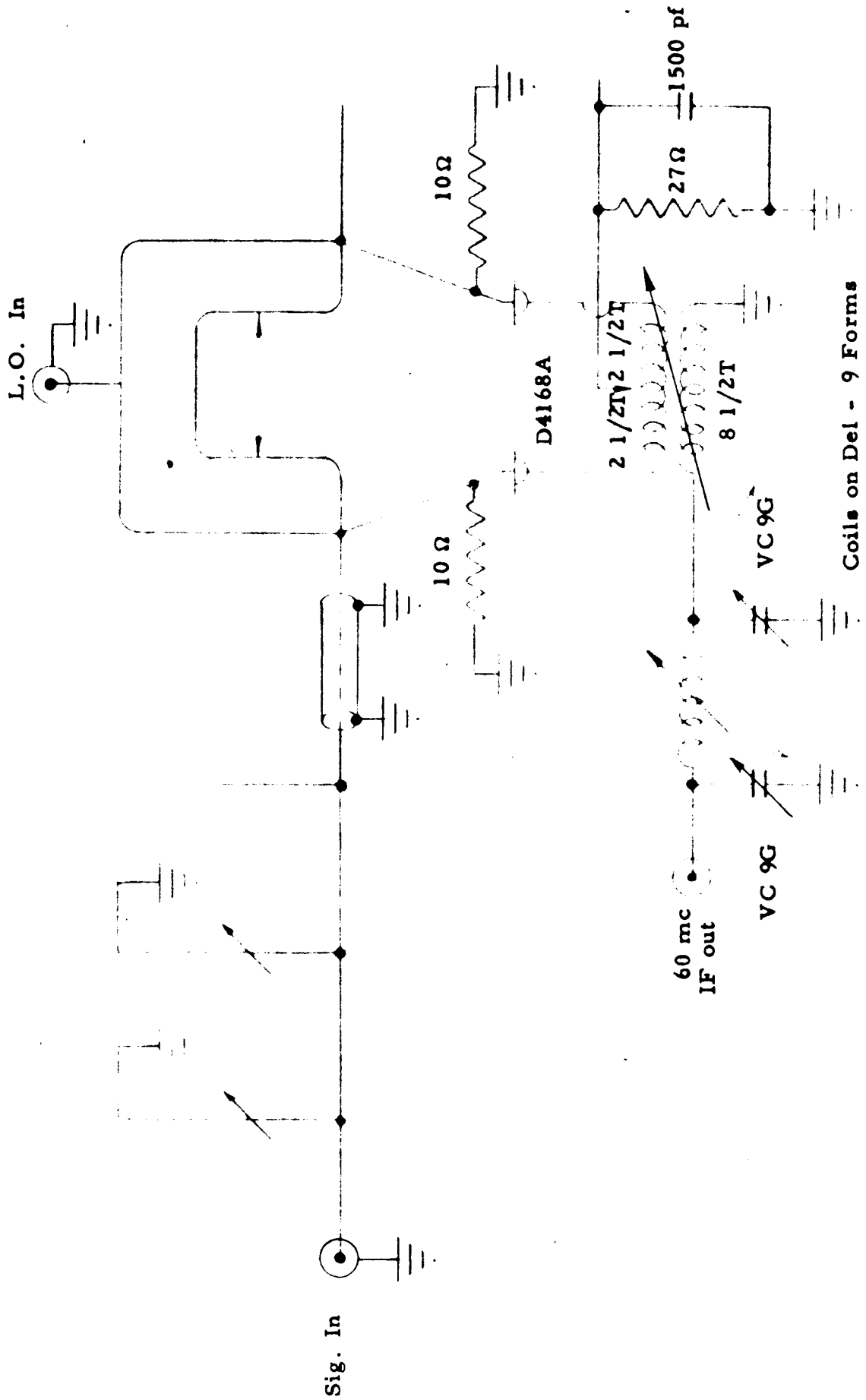


FIG. 12 MICRO-STRIP BALANCED TD DOWNCONVERTER



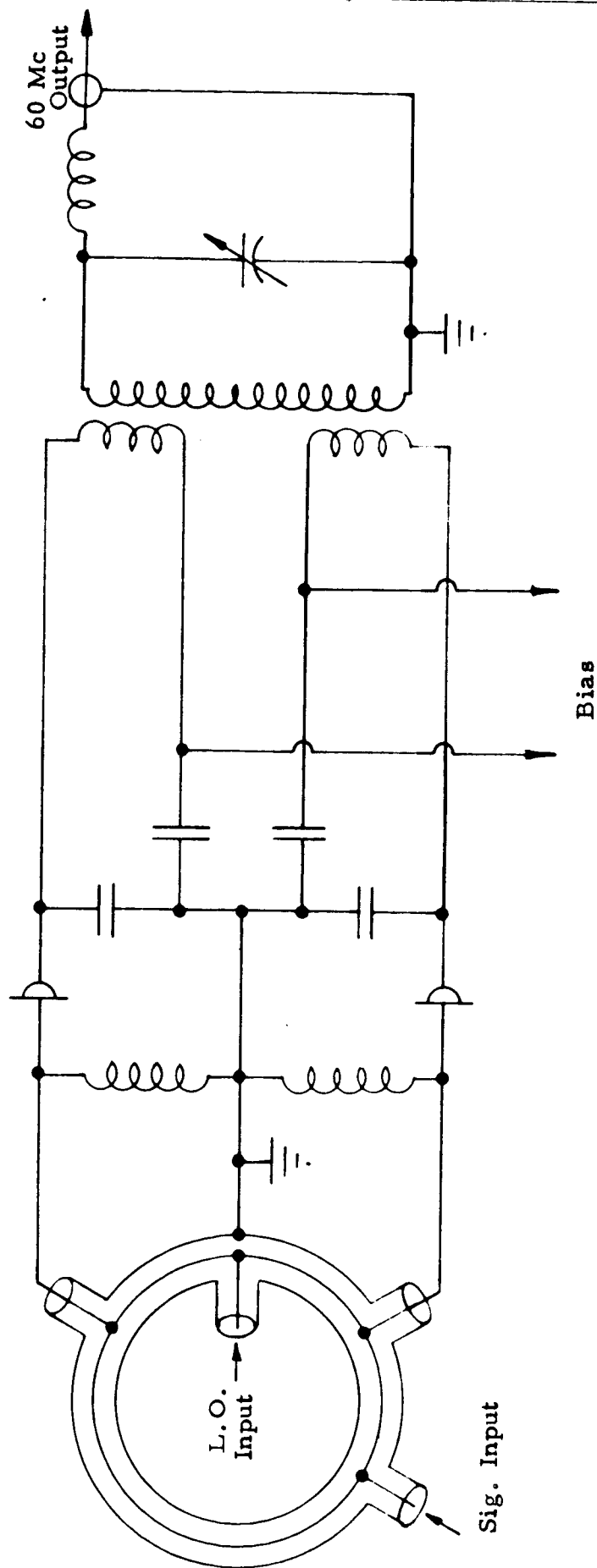


FIG. 13 BALANCED COAXIAL DOWNCONVERTER

Aside from the coaxial ring, the construction employed was a combination of strip line and conventional lumped constant construction. The device was operated in conjunction with an LEL 60 Mc IF amplifier having a gain of 40 db and a noise figure of <2.5 db.

The results were disappointing. The best sensitivity, using a criterion of $S+N/N = 2$ at 60 Mc on a spectrum analyzer, was -103 dbm, which is slightly inferior to what can be obtained with a high quality balanced diode mixer.

Two conclusions were reached: 1) that little was to be gained by balanced operation until a good sensitivity and noise figure could be obtained with a single TD circuit, and 2) that diode instability was preventing operation at the optimum point on the negative conductance region of the TD curve.

Two widely accepted approximate criteria for tunnel diode stability are

$$R < |-r| \quad \text{to avoid switching} \quad (37)$$

$$R > \frac{L}{rC} \quad \text{to avoid oscillation} \quad (38)$$

where

R = total positive resistance in the loop including the diode
ohms

$-r$ = negative resistance of the diode, ohms

L = total inductance in the loop, henries

C = diode junction capacitance, farads.

With D4168 A diodes, it appeared that the 50Ω impedance seen by the diode looking toward the hybrid ring should stabilize the circuit if inductance could be kept low enough. It was decided, therefore, to construct a single diode strip line circuit to minimize inductance.

3.2.3 Strip Line Version

Figure 14 shows the strip line circuit employed with a single tunnel diode. As constructed, three layers of double copper faced Rexolene P were used, with the diode located in a hole in the center layer. The shorted $\lambda/4$ stub at signal frequency provides a dc return for the diode and is essentially a short at the 60 Mc IF frequency. The open $\lambda/4$ stub provides a low impedance path for oscillator and signal and is essentially open circuited at the IF frequency.

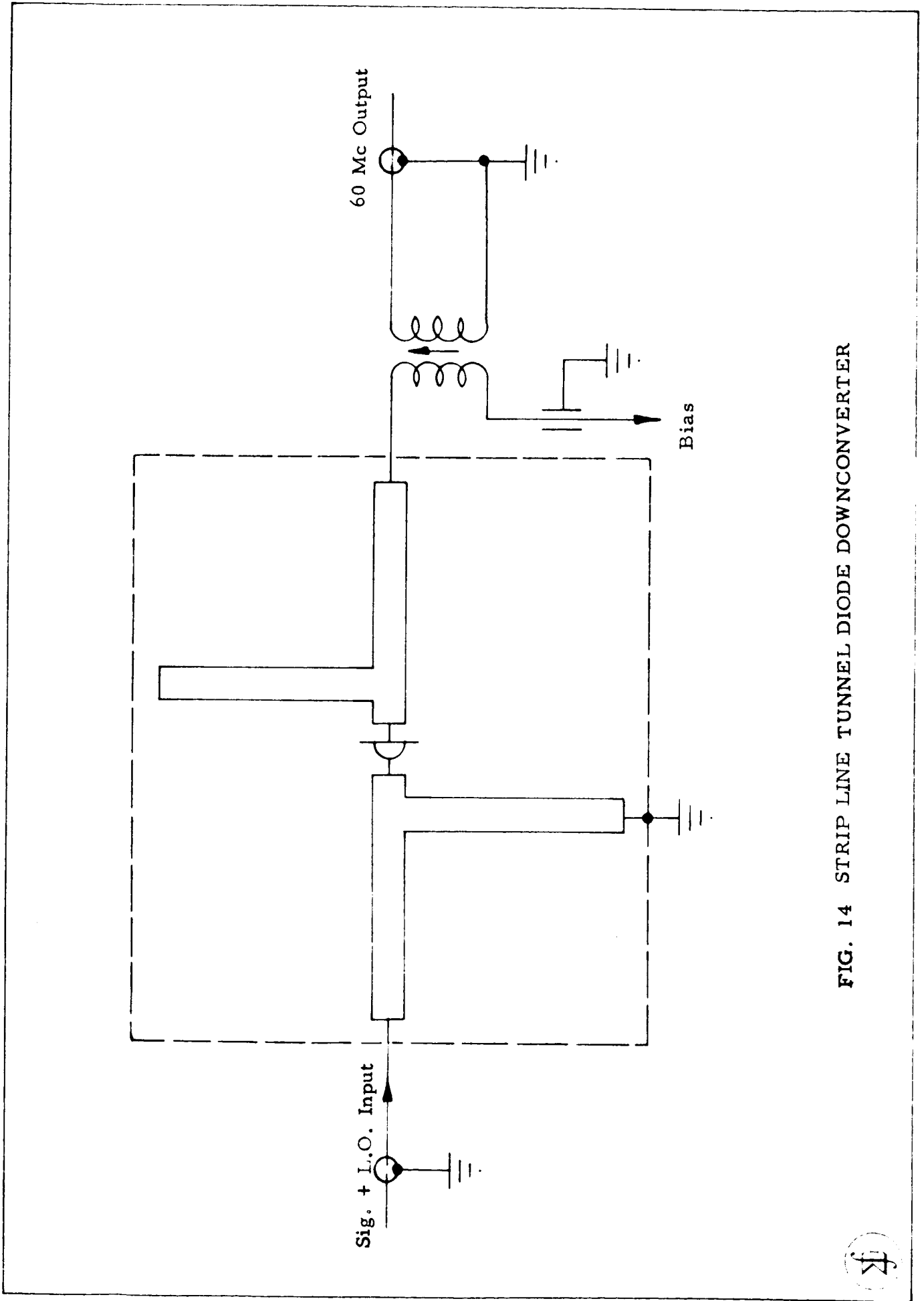


FIG. 14 STRIP LINE TUNNEL DIODE DOWNCONVERTER



This strip line circuit was fabricated and tested at both 1610 Mc and 2113 Mc. The latter unit was constructed because of the availability of circulators at that frequency. The physical appearance is shown in Fig. 15, and the method of mounting the diode in Fig. 16.

The coaxial ring hybrid was employed for L.O. insertion and isolation with the unused port terminated in $50\ \Omega$. This added 3 db to the measured noise figure.

With this circuit, the maximum sensitivity observed at 1610 Mc was -107 dbm and the best double side-band noise figure (corrected for hybrid loss) was 9 db. These results were obtained with a local oscillator input at 1550 Mc of 0.5 mw and with the tunnel diode biased just beyond the valley point. Somewhat poorer noise figure resulted with biasing just below the peak value.

The 2113 Mc unit yielded a dsb noise figure of 10.5 db and a sensitivity of -105 dbm.

For comparison purposes, a 1610 Mc Trak balanced mixer using 1N21F diodes with a 3 db directional coupler type hybrid measured 10.5 db dsb noise figure. This unit required 5.5 mw local oscillator power for best noise figure, or roughly ten times as much power as the 1610 Mc tunnel diode unit.

All noise figure measurements included the contribution of the LEL 60 Mc IF amplifier.

3.2.4 Observations

While the TD down-conversion approach was dropped, several worthwhile observations were noted.

a) Noise figures comparable to, or slightly better, than those achieved with good quality resistive diodes can be obtained at L and S-band. The D4168A diodes used have a cut-off frequency of about 7 Gc. Better results could be achieved with higher cut-off diodes. Moreover, some improvement would probably result from a balanced configuration.

b) Stability with tunnel diodes is a difficult problem. Even the low inductance strip line construction did not completely eliminate oscillation at some bias values.

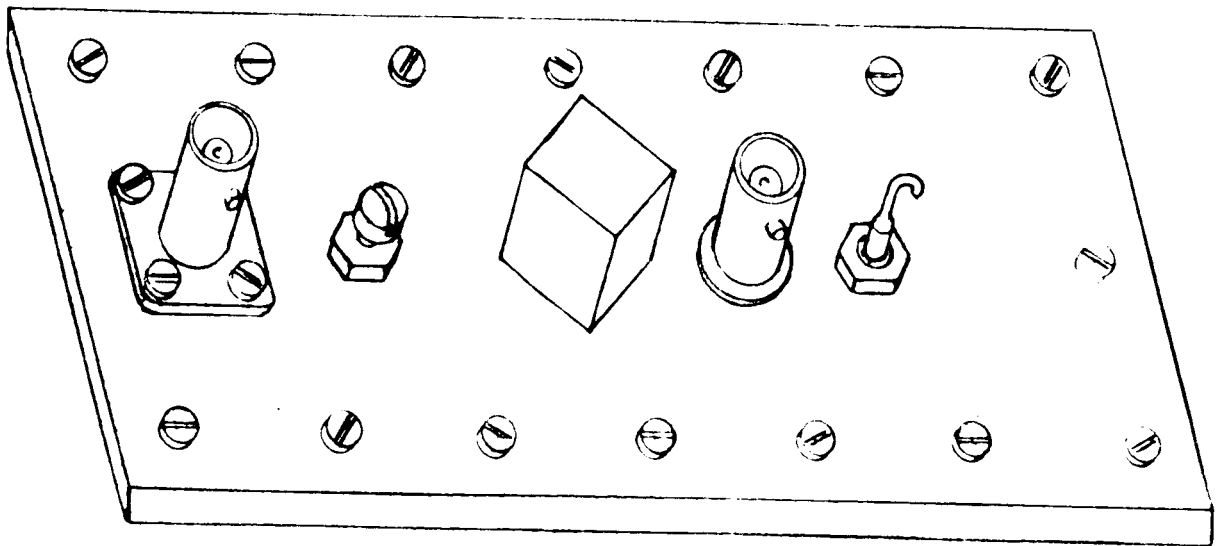
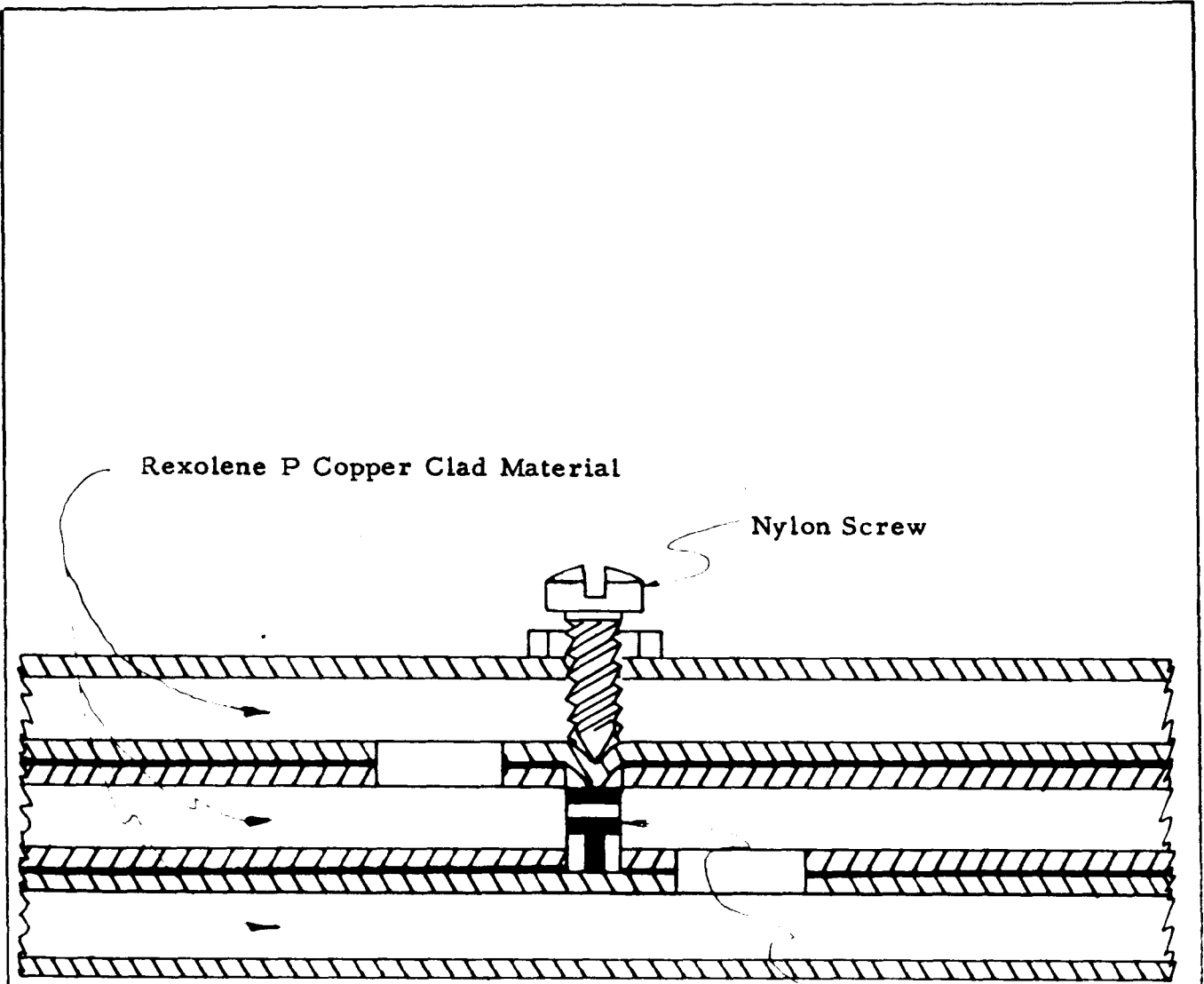


FIG. 15 STRIP LINE DOWNCONVERTER





Tunnel Diode

FIG. 16 DIODE MOUNTING FOR STRIP LINE
DOWNCONVERTER



c) Bias and local oscillator drive levels are critical for optimum noise figure.

d) Considerable variability exists in tunnel diode characteristics. Optimum operation can best be achieved with access to a large supply of diodes for selection.

e) Operation with a circulator or isolator seems to be indicated for good stability. Accurate noise figure measurement requires stable impedance.

f) While the tunnel diode has superior steady-state burnout characteristics, it is subject to damage by transients.

4. REVIEW OF PHASE STABILITY MEASUREMENT PROCEDURES

A re-examination of the phase stability measuring system described in our report of March 1963 under Contract NAS 8-1643 has provided a better knowledge of the system limitations and extended its application by a more general analysis.

4.1 Description

The phase stability measuring system as it is now being used by SEI consists of the balanced system shown in Fig. 11. A hybrid network is used whereby the energy contained in the signal may be cancelled leaving only the energy outside the center frequency of the signal. De-modulation of the energy outside the center frequency results in a spectrum with the center frequency translated to zero frequency. This spectrum may be analyzed by conventional means and yields what is termed as frequency domain measurements.

4.2 Analysis of System

Referring to Fig. 17, the signals out of the hybrid for matched conditions are:

$$E_A = \frac{E_1' + E_2' e^{j0}}{2} \quad (39)$$

$$E_B = \frac{E_1' + E_2' e^{j(180+0)}}{2} \quad (40)$$

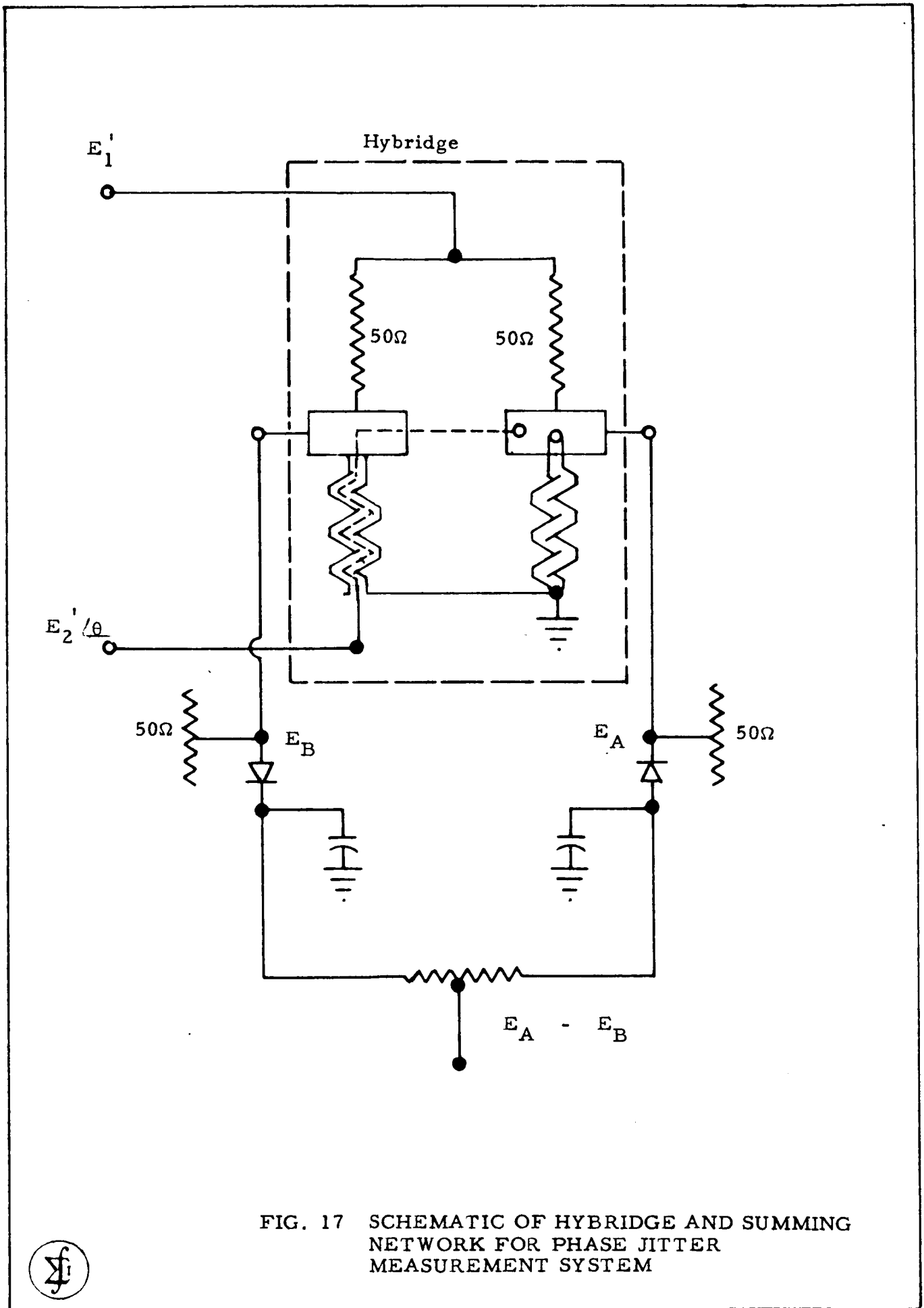


FIG. 17 SCHEMATIC OF HYBRIDGE AND SUMMING NETWORK FOR PHASE JITTER MEASUREMENT SYSTEM



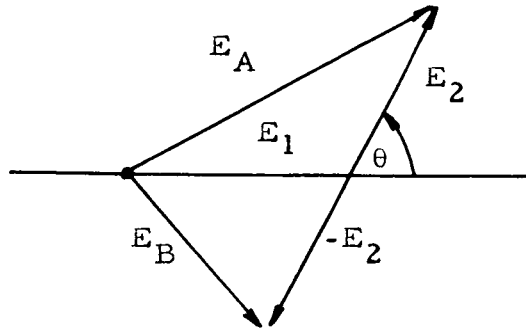
letting

$$E_1'/2 = E_1 \quad \text{and} \quad E_2'/2 = E_2$$

$$E_A = E_1 + E_2 (\cos \theta + j \sin \theta) \quad (41)$$

$$E_B = E_1 - E_2 (\cos \theta + j \sin \theta) \quad (42)$$

After linear detection the magnitude of E_A and E_B are



$$|E_A| = [E_1^2 + E_2^2 + 2 E_1 E_2 \cos \theta]^{1/2} \quad (43)$$

$$|E_B| = [E_1^2 + E_2^2 - 2 E_1 E_2 \cos \theta]^{1/2} \quad (44)$$

Rewriting Eq. 43, and 44

$$|E_A| = [a + 2b \cos \theta]^{1/2} \quad (45)$$

$$|E_B| = [a - 2b \cos \theta]^{1/2} \quad (46)$$

where $a = E_1^2 + E_2^2$

$$b = E_1 E_2$$

and with $\theta = \frac{\pi}{2} + \Delta\theta$ radians

expansion by Taylor Series yields

$$|E_A| = \sqrt{a} - \frac{b}{\sqrt{a}} \Delta\theta \left[1 + \frac{b}{2a} \Delta\theta - \left(\frac{1}{6} - \frac{b^2}{2a^2} \right) \Delta\theta^2 - \frac{b}{a} \left(\frac{1}{6} - \frac{5b^2}{8a^2} \right) \Delta\theta^3 + \dots \right] \quad (47)$$

$$\begin{aligned} |E_B| = \sqrt{a} + \frac{b}{\sqrt{a}} \Delta\theta & \left[1 - \frac{b}{2a} \Delta\theta - \left(\frac{1}{6} - \frac{b^2}{2a^2} \right) \Delta\theta^2 \right. \\ & \left. + \frac{b}{a} \left(\frac{1}{6} - \frac{5b^2}{8a^2} \right) \Delta\theta^3 + \dots \right] \end{aligned} \quad (48)$$

Then

$$|E_A| - |E_B| = -\frac{b}{\sqrt{a}} \Delta\theta \left[2 - \left(\frac{1}{3} - \frac{b^2}{a^2} \right) \Delta\theta^2 + \dots \right] \quad (49)$$

$$|E_A| + |E_B| = 2\sqrt{a} - \frac{b^2}{a^{3/2}} \Delta\theta^2 \left[1 - \left(\frac{1}{3} - \frac{5b^2}{4a^2} \right) \Delta\theta^2 + \dots \right] \quad (50)$$

Replacing a and b with their equivalents, Eq. 49 becomes:

$$|E_A| - |E_B| = \frac{E_1 E_2}{\sqrt{E_1^2 + E_2^2}} \Delta\theta \left\{ 2 - \left[\frac{1}{3} - \left(\frac{E_1 E_2}{E_1^2 + E_2^2} \right)^2 \right] \Delta\theta^2 + \dots \right\} \quad (51)$$

4.3 Observations

The jitter measuring system of Fig. 11 is among the simplest systems used in frequency domain measurements. The value of phase jitter $\Delta\theta$ may be estimated from the first order terms in Eq. 51.

From Eq. 51

$$\Delta\theta = \frac{\sqrt{E_1^2 + E_2^2}}{2 E_1 E_2} \left(|E_B| - |E_A| \right) \quad (52)$$

if E_1 and E_2 were the same this would reduce to

$$\Delta\theta = \frac{|E_B| - |E_A|}{\sqrt{2} E_1} \quad (53)$$

The maximum value of $\Delta\theta$ thus obtained would represent the maximum phase jitter occurring when the rate of change of θ is within the bandpass of the system.

With a more elaborate measurement system, perhaps involving multipliers, filters and mixers, it would be possible to plot the phase jitter versus frequency $\left(\frac{d\theta}{dt} \right)$.

The $\Delta\theta$ term in Eq. 51 will ordinarily be a random function of time and produce a frequency spectrum. By displacing the magnitude of the $\Delta\theta$ term on a scope and measuring the peak to peak response, an indication of the phase instability or jitter is obtained. The value of this peak to peak response we have called $|E_B| - |E_A|$ and assume it related to $\Delta\theta$ by Eq. 51. The value of $\Delta\theta$ we have called the phase jitter. If the test units, Fig. 11, contribute equal amounts of jitter, it would be expected that the jitter of an individual test unit would be $\frac{\Delta\theta}{\sqrt{2}}$.

An important aspect of the phase stability measurement system of Fig. 11 is that jitter from the oscillator should not appear in the output of the system $(|E_A| - |E_B|)$. This would first require that any dispersion in the oscillator jitter spectrum introduced by the test units be identical. If E_1 and E_2 contain peak amplitude variations of ΔE it may be shown, by differentiation of Eq. 51 that these variations will cause a variation of approximately $\sqrt{2} \Delta E \Delta\theta$ in $|E_A| - |E_B|$ which in turn relate to error in the value of $\Delta\theta$. Since ΔE will normally be very small, the term $\Delta E \Delta\theta$ becomes second order compared to $\Delta\theta$.

It would seem that low frequency components in the output represent relatively long term instabilities and high frequency components represent relatively short term instabilities, however, the lack of knowledge of component frequencies will prevent desired correlation between frequency and term stability.

The phase indicated on the scope represents the maximum phase deviation within the passband of the system.

In conclusion, the jitter measuring system of Fig. 11 will provide an indication of the relative phase stability between different test units. However, because this system produces no type of spectral data, it would not be possible to state jitter in terms of statistical quantities.

5. SUMMARY

During the twelve-month reporting period, the theoretical study of frequency division has yielded the important concept that "true" division requires storage time, and that practical dividers actually lock a subharmonically related output to some parameter of the input signal. Moreover, signal-to-noise enhancement by true frequency division has been shown to be impossible, although certain practical approaches could conceivably offer some improvement. A significant experimental result was the discovery that step-recovery diodes can be used as highly efficient subharmonic generators.

The parametric amplifier portion of the RF amplifier program resulted in a summary of the characteristics of the various standard types and the factors influencing the choice between types in given applications. Moderately successful tunnel diode down-conversion was achieved at L- and S-band. It was concluded that the advantages to be achieved by tunnel diode mixing would often be outweighed by the difficulty of obtaining stability, the variation in diode characteristics, the critical adjustment for optimum performance, and the danger of transient burnout.

Review of the SEI phase stability measurement procedure confirmed the usefulness of the approach while pointing out the difficulty of extracting all the desirable information from the measurements.

6. RECOMMENDATIONS

It is clear that the theory of frequency division needs further study, both with respect to the search for optimum devices and the more complete understanding of the mechanism of the step-recovery subharmonic generator.

It is also apparent that the step-recovery diode should be extremely useful in other types of frequency-changing devices, and that its application to various frequency synthesis and solid-state power generation problems should be explored.

The measurement of phase-stability and correlation with other short-term stability concepts needs further study.

7. REFERENCES

1. James, Nichols & Phillips, "MIT Radiation Laboratory Series", vol. 25, p 284.
2. Davenport, W. B. and W.L. Root, "An Introduction to the Theory of Random Signals & Noise", McGraw-Hill, 1958, p. 62, 104.
3. Lee, Y.W., "Statistical Theory of Communication", John Wiley & Sons, 1960, pp. 221-224.
4. Manley, J.M. and H.E. Rowe, "Some General Properties of Non-Linear Elements - Part 1, General Energy Relations", Proc. IRE, July 1956, pp 904 ff.
5. Penfield, P. Jr., "Frequency Power Formulas", MIT, Tech. Press and John Wiley & Sons, N.Y. 1960.
6. Weiss, M.T., "Quantum Derivation of Energy Relations Analogous to those for Non-Linear Reactances", Proc. IRE, vol. 45, No. 7, July 1957, p. 1012.
7. Hefni, I., "The Negative Resistances in Junction Diodes", Proc. IRE, vol. 49, Sept. 1961, pp 1427-1428.
8. McDade, J.C., "Explanation of One Type of RF Induced Negative Resistance in Junction Diodes", Proc. IRE, vol. 50, Jan. 1962 p. 91.